UNIVERSITÄT HEIDELBERG
ZUKUNFT
SEIT 1386

UNIVERSITÄT HEIDELBERG
Physikalisches Institut

F20 MOT
(Fortgeschrittenen-Praktikum Versuch F20: Magnetooptische Falle)
-
Preparatory Material

F20 Tutors

vorlesung-weidemueller@physi.uni-heidelberg.de

March 5, 2014

Contents

History

- 2014/03/05 First version of pdf document, fully syncronized with wiki. (V. Gavryusev)

In autumn 2009 the magneto-optical trap of the F20 experiment was completely revised, improved and adapted to high safety standards. This included a complete renewal of the experimental setup which was done by Marc Repp, Christoph Hofmann, Silvânia Alves de Carvalho, Kristina Meyer, and Dominic Litsch.

A new and interactive lab manual in form of a wikipedia was established by Christoph Hofmann and Marc Repp. Then it was updated by Vladislav Gavryusev. This pdf version is the full mirror of the contents of the wiki.

Introduction

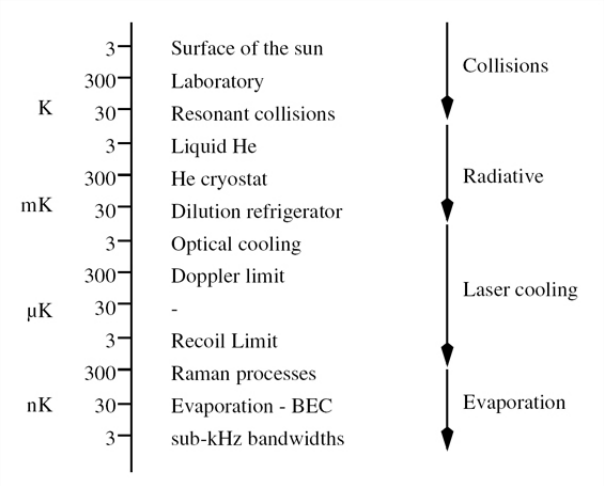

Figure 1: Temperature scale. (Taken from [1])

The idea to use laser radiation to cool and trap atoms was first suggested by Wineland and Dehmelt [2] and independently by Hänsch and Schawlow [3]. Since photons carry momentum, the momentum exchange between the laser radiation and the atoms in an absorption process can be used to apply a force on the atoms. Since the absorption depends on the difference between frequency of the laser radiation and the absorption frequency of the atoms, the absorption process can be made velocity-selective due to the Doppler effect, which shifts the atoms absorption frequency depending on its velocity. It is this simple notion that forms the basis for the research that has been carried out in the last 30 years in the field of laser cooling and trapping. Especially the velocity dependence of the process, leading to the fact that the forces are no longer conservative but can instead dissipate kinetic energy of the atoms, allows the experimentalists to cool atoms down to extremely low temperatures bridging more than more than nine orders of magnitude on the temperature scale!

During the course of this week's experiment you will lower the temperature of hot Rubidium atoms of several $100K$ down to at least several $100\mu K$, thereby crossing as many as seven orders of magnitude. In the same time you will learn how to realize one of the most important laser cooling experiments carried out in modern Atomic Physics. As you might know, a magneto-optical trap (MOT) is the first step towards the formation of ultracold quantum gases. And it is a technique which is used on a daily basis also here in Heidelberg, where a whole variety of alkali atoms are trapped in the groups of Prof. Matthias Weidemuller (Lithium, Rubidium, Caesium), Prof. Selim Jochim (Lithium) and Prof. Markus Oberthaler (Lithium, Sodium, Rubidium, Argon).

Before you can get started, you have to acquaint yourself with the topics listed below:

- Of course no lab course can be successfully carried out without Theory (§ 1-2).
- But for an experimentalist, Theory is only part of the story. He wants to verify or falsify the Theory by doing experiments. Therefore he needs an Experimental setup (§ 3).
- Before you can enter the lab you need to familiarize yourself with several Safety issues (§ 4.1), which we will also discuss during our colloquium at the beginning of the lab course.
- After having read all the above pages and after having passed the small colloquium, it is up to you: **Hands on!** To do so, please read the Work instructions carefully (§ 4.2).
- Last, but not least you should analyze the acquired data and report your results. These Data Analysis instructions will help you (§ 4.3).

Chapter 1

Spectroscopy

Saturated absorption experiments were awarded the 1981 Nobel prize in physics (Nicolaas Bloembergen and Arthur L. Schawlow) and related techniques have been used in laser cooling and trapping experiments, leading to the 1997 Nobel prize (Steven Chu, Claude Cohen-Tannoudji, and William D. Phillips), and then the achievement of Bose-Einstein condensation was recognized with the 2001 Nobel prize (Eric A. Cornell, Wolfgang Ketterle, and Carl E. Wieman). Although the basic principles are straightforward, you will only be able to unleash the full power of saturated absorption spectroscopy by carefully considering many details that will be discussed in this first theory section.

1.1 Basic laser absorption spectroscopy

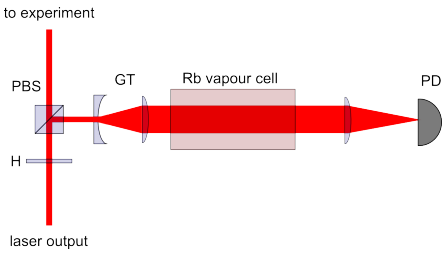

Figure 1.1: Schematic sketch of a spectroscopy path allowing for Doppler spectroscopy: PBS = polarizing beam splitter, GT = Galilean Telescope, H = half waveplate.

The basic arrangement for ordinary laser absorption (not saturated absorption spectroscopy) through a gaseous sample is shown in Fig. 1.1. A

laser beam passes through the vapor cell and its intensity is measured by a photo diode detector as the laser frequency ν is scanned through the natural resonance frequency. When a laser beam propagates through a gaseous sample, the two stimulated transition processes change the intensity of the laser beam and affect the density of atoms (number per unit of volume) in the ground and excited states. Additionally, Doppler shifts associated with the random thermal motion of the absorbing atoms must be taken into account. There is an interplay among these effects which is critical to understanding saturated absorption spectroscopy. We begin with the basic equation describing how the laser intensity changes as it propagates through the sample and then we'll continue with the effects of Doppler shifts and population changes.

Because of stimulated emission and absorption, the laser intensity $I(x)$ varies as it propagates from x to $x + dx$ in the medium. This gives rise to the well known Lambert-Beer absorption law

$$\frac{dI}{dx} = -\kappa I \tag{1.1}$$

with the absorption coefficient (fractional absorption per unit length)

$$\kappa = h\nu n_0 \alpha \left(P_0 - P_1\right) \tag{1.2}$$

Here

$$\alpha = \alpha_0 \mathcal{L}(\nu, \nu_0) \tag{1.3}$$

and

$$\mathcal{L}(\nu, \nu_0) = \frac{1}{1 + 4(\nu - \nu_0)^2/\Gamma^2} \tag{1.4}$$

give the Lorentzian (or natural resonance) frequency dependence.

The proportionality to $P_0 - P_1$ arises from the competition between stimulated emission and absorption and it is important to appreciate the consequences. If there are equal numbers of atoms in the ground and excited state ($P_0 - P_1 = 0$), laser photons are as likely to be emitted by an atom in the excited state as they are to be absorbed by an atom in the ground state and there will be no attenuation of the incident beam. The attenuation is maximized when all atoms are in the ground state ($P_0 - P_1 = 1$) because only absorption would be possible. And the attenuation can even reverse sign (becoming an amplification as it does in laser gain media) if there are more atoms in the excited state ($P_1 > P_0$).

In the absence of a laser field, the ratio of the atomic populations in the two energy states will thermally equilibrate at the Boltzmann factor $P_1/P_0 = exp\{-\Delta E/k_B T\} = exp\{-h\nu_0/k_B T\}$. At room temperature, $k_B T \approx 1/40eV$

is much smaller than the energy difference between the levels involved in this experiment $h\nu_0 \approx 1.6eV$ and nearly all atoms will be in the ground state, i.e., $P_0 - P_1 = 1$. While you will see shortly how the presence of a strong laser field can significantly perturb these thermal equilibrium probabilities, for now we will only treat the case where the laser field is weak enough that $P_0 - P_1 = 1$ remains a good approximation throughout the absorption cell.

1.2 Doppler shifts

Atoms in a vapor cell move randomly in all directions with each velocity component having a distribution of values. Only the velocity component parallel to the laser beam direction will be important when taking into account Doppler shifts and it is this component that we refer to with the symbol v. The density of atoms dn in the velocity group between v and $v + dv$ is given by the Boltzmann velocity distribution:

$$dn = n_0 \sqrt{\frac{m}{2\pi k_B T}} e^{-mv^2/2k_B T} dv \tag{1.5}$$

With a standard deviation (proportional to the width of the distribution) given by:

$$\sigma_v = \sqrt{\frac{k_B T}{m}} \tag{1.6}$$

this is just a standard Gaussian distribution

$$dn = n_0 \frac{1}{\sqrt{2\pi}\sigma_v} e^{-v^2/2\sigma_v^2} dv \tag{1.7}$$

with a mean of zero - indicating that the atoms are equally likely to be going in either direction. Note that the distribution's variance σ_v^2 increases linearly with temperature and decreases inversely with atomic mass.

Atoms moving with a velocity v see the laser beam Doppler shifted by the amount $\nu(v/c)$. We will take an equivalent, alternate view that atoms moving with a velocity v have a Doppler shifted resonance frequency

$$\nu_0' = \nu_0 \left(1 + \frac{v}{c}\right) \tag{1.8}$$

in the lab frame. The sign has been chosen to be correct for a laser beam propagating in the positive direction, so that the resonance frequency is blue shifted to higher frequencies if the velocity is positive and red shifted if the velocity is negative.

The absorption coefficient $d\kappa$ from a velocity group dn at a laser frequency ν is then obtained from Eq. 1.2 by substituting dn for n_0 and by adjusting the Lorentzian dependence of α (Eq. 1.3) so that it is centered on the Doppler shifted resonance frequency ν_0' (keeping its dependence on v in mind through Eq. 1.8):

$$d\kappa = h\nu\alpha_0 \left(P_0 - P_1\right) \mathcal{L}(\nu, \nu_0')dn \tag{1.9}$$

Introducing the velocity dependence of dn (Eq. 1.5) and accounting for the weak laser field case ($P_0 - P_1 = 1$) yields:

$$d\kappa = n_0 h\nu\alpha_0 \sqrt{\frac{m}{2\pi k_B T}} \mathcal{L}(\nu, \nu_0') e^{-mv^2/2k_B T} dv \tag{1.10}$$

The absorption coefficient from all atoms is then found by integrating over all velocity groups:

$$\kappa = \kappa_0 e^{-(\nu-\nu_0)^2/2\sigma_\nu^2} \tag{1.11}$$

with the width parameter given by

$$\sigma_v = \nu_0 \sqrt{\frac{k_B T}{mc^2}} \tag{1.12}$$

and

$$\kappa_0 = n_0 h\nu\alpha_0 \sqrt{\frac{m}{2\pi k_B T}} \frac{c}{\nu_0} \frac{\pi\Gamma}{2} \tag{1.13}$$

The frequency dependence of the absorption coefficient is shown in Fig. 1.2.

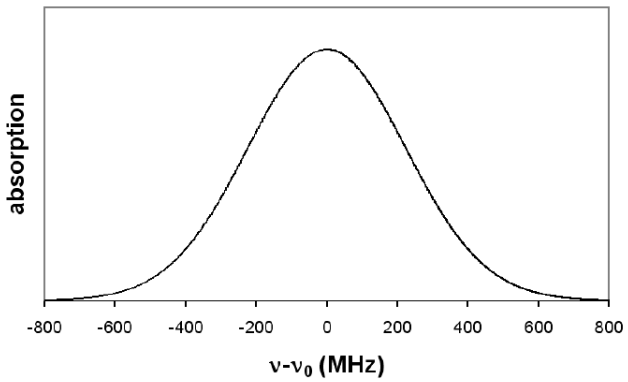

Figure 1.2: Doppler profile. The absorption coefficient vs. the laser frequency offset from resonance has a Gaussian lineshape.

1.3 Populations

Now we would like to take into account the changes to the ground and excited state populations arising from a laser beam propagating through the cell. The rate equations for the ground and excited state probabilities become:

$$\frac{dP_0}{dt} = \gamma P_1 - \alpha I \left(P_0 - P_1\right) \tag{1.14}$$

$$\frac{dP_1}{dt} = -\gamma P_1 + \alpha I \left(P_0 - P_1\right) \tag{1.15}$$

where the first term on the right in each equation arises from spontaneous emission with rate γ and the second term arises from stimulated absorption and emission. The steady state of the above two level system then obeys:

$$P_0 - P_1 = \frac{1}{1 + 2\alpha I/\gamma} \tag{1.16}$$

which is now dependent of the laser power. This fact of course also influences the absorptive behavior of the sample and results in an intensity dependent absorption coefficient:

$$\kappa = \kappa_0' e^{-(\nu-\nu_0)^2/2\sigma_\nu^2} \tag{1.17}$$

where the width parameter, σ_ν) is the same as before (see Eq. 1.12), but compared to the weak-field absorption coefficient derived in Eq. 1.13, the strong-field coefficient decreases to

$$\kappa_0' = \frac{\kappa_0}{\sqrt{1 + 2I/I_{sat}}} \tag{1.18}$$

Here I_{sat} is called the **saturation intensity**

$$I_{sat} = \frac{\gamma}{\alpha} \tag{1.19}$$

and is about $1.6 mW/cm^2$ for our Rubidium transitions.

1.4 Saturated absorption and Doppler free spectroscopy

Up to now, we have considered only a single laser beam propagating through the cell. Now we would like to understand what happens if a second laser propagates through the cell in the opposite direction. This is the basic arrangement for saturated absorption spectroscopy shown in Fig. 1.3. The

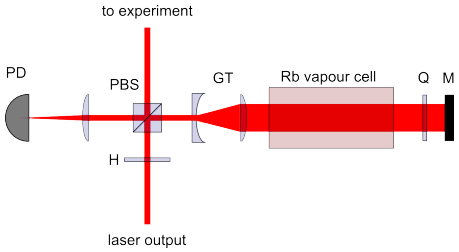

Figure 1.3: Schematic sketch of a spectroscopy path allowing for Doppler free saturated absorption spectroscopy. PBS = polarizing beam splitter, GT = Galilean Telescope, H = half waveplate, Q = quarter waveplate, M = mirror

laser beam traveling to the right is called the pump beam. The second, retro-reflected laser beam propagating in the opposite direction is called the probe beam.

With only a single weak laser propagating through the sample, $P_0 - P_1 = 1$ would be a good approximation throughout the cell. To do saturated absorption spectroscopy the probe beam will still be kept weak enough to neglect its effect on the populations. However, the pump beam will be made strong - strong enough to significantly affect the populations and thus change the measured absorption of the probe beam. To understand how this comes about, we will again have to consider Doppler shifts.

As mentioned, the stimulated emission and absorption rates are non-zero only when the laser is near the resonance frequency. Thus, we will obtain $P_0 - P_1$ from Eq. 1.16 by giving α a Lorentzian dependence on the Doppler shifted resonance frequency:

$$\alpha = \alpha_0 \mathcal{L}(\nu, \nu_0'') \tag{1.20}$$

with the important feature that for the pump beam, the resonance frequency for atoms moving with a velocity v is

$$\nu_0'' = \nu_0 \left(1 - \frac{v}{c}\right) \tag{1.21}$$

This frequency is Doppler shifted in the opposite direction to that of the probe beam because the pump beam propagates through the vapor cell in the negative direction. That means that the resonant frequency for an atom moving with velocity v is $\nu_0 (1 + v/c)$ for the probe beam and $\nu_0 (1 - v/c)$ for the pump beam.

For large detunings $\delta \gg \Gamma$, $P_0 - P_1 = 1$ implying that in this case the atoms are in the ground state. On resonance, i.e., at $\delta = 0$, $P_0 - P_1 = 1/(1 + 2I/I_{sat})$, which approaches zero for large values of I. This means that

atoms in resonance with a strong pump beam will have equal populations in the ground and excited states ($P_0 - P_1 = 0$). In other words, a strong resonant laser field causes such rapid transitions in both directions that the two populations equilibrate. Such laser beam is then said to "saturate" the transition, which is the origin of the name of the technique.

According to Eq. 1.21, the resonance condition $\delta = 0$ translates to $v = v_{pump}$ where

$$v_{pump} = c\left(1 - \frac{\nu}{\nu_0}\right) \tag{1.22}$$

Consequently, for any frequency ν within the Doppler profile, only atoms near this velocity will be at zero detuning and will have values of $P_0 - P_1$ perturbed from the "pump off" value of unity.

The density of atoms in the ground state $dn_1 = P_1 dn$, plotted as a function of the velocity, will follow the Maxwell-Boltzmann distribution except very near $v = v_{pump}$ where it will drop off significantly as atoms are promoted to the excited state. This is called "hole burning" as there is a hole (a decrease) in the density of atoms in the ground state near $v = v_{pump}$ (and a corresponding increase in the density of atoms in the excited state) as demonstrated in Fig. 1.4.

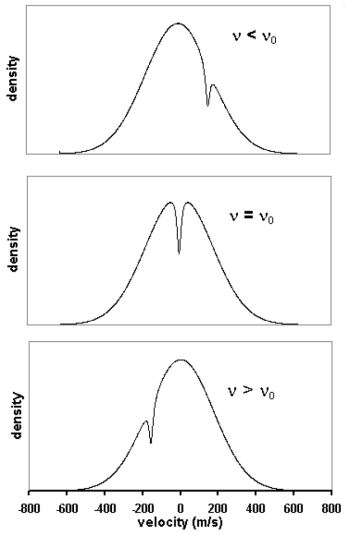

Figure 1.4: Hole burning by the pump beam. The density of ground state atoms is plotted vs. their velocity and becomes depleted near the velocity that Doppler shifts the laser frequency into resonance with ν_0.

How does hole burning affect the probe beam absorption? You learned

that the absorption at any frequency ν arises only from those atoms moving with velocities near $v_{probe} = c\,(\nu/\nu_0 - 1)$. Also recall that the probe beam absorption is proportional to $P_0 - P_1$, which we have just seen remains constant (≈ 1) except for atoms having nearly the exact opposite velocities near $v_{pump} = c\,(1 - \nu/\nu_0)$. Therefore, when the laser frequency is far from the natural resonance ($|\nu - \nu_0| \gg \Gamma$) , the probe absorption arises from atoms moving with a particular velocity in one direction while the pump beam is burning a hole for a completely different set of atoms with the opposite velocity. In this case, the presence of the pump beam will not affect the probe beam absorption which would follow the standard Doppler-broadened profile.

Only when the laser frequency is very near the resonance frequency ($\nu = \nu_0$, $v_{probe} = v_{pump} = 0$) the pump beam will burn a hole for atoms with velocities near zero which would then be the same atoms involved in the absorption of the probing beam at this frequency. The absorption coefficient would be obtained by taking $P_0 - P_1$ as given by Eq. 1.16 (with Eqs. 1.20 and 1.21) to be a function of the laser frequency and the velocity, using it in Eq. 1.9 (with Eqs. 1.5 and 1.8), and then integrating over velocity. The result is a Doppler-broadened profile with what's called a **saturated absorption dip** (or **Lamb dip**) right at $\nu = \nu_0$. Numerical integration was used to create the profiles shown in Fig. 1.5 for several values of I/I_{sat}. As one can see, increasing the intensity leads to the so called **power broadening** of the Lamb dip.

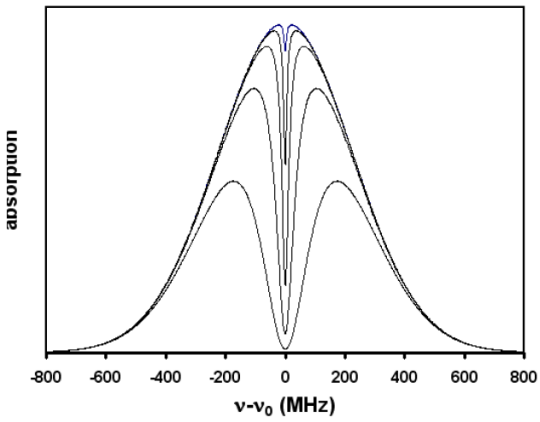

Figure 1.5: Absorption coefficient vs. the laser frequency offset from resonance for a two-level atom at values of $I/I_{sat} = 0.1$; 1; 10; 100; 1000 (from smallest dip to largest). It shows a Gaussian profile with the saturated absorption dip at $\nu = \nu_0$.

1.5 Multilevel effects

Real atoms have multiple upper and lower energy levels which add complexities to the simple two-level model presented so far. In the spectroscopy cell, transitions between two lower levels and four upper levels can all be reached with our laser and add features called crossover resonances and a process called optical pumping. Crossover resonances are additional narrow absorption dips arising because several upper or lower levels are close enough in energy that their Doppler-broadened profiles overlap. Optical pumping occurs when the excited level can spontaneously decay to more than one lower level. It can significantly deplete certain ground state populations further enhancing or weakening the saturated absorption dips.

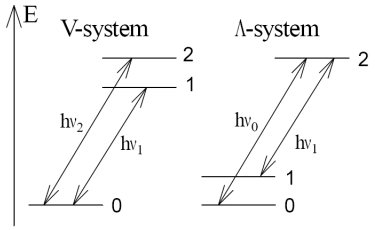

Figure 1.6: Energy levels for two possible three level systems. The V-configuration with two upper levels and the Λ-system with two lower levels.

The basics of crossover resonances can be understood within the three-level atom in either the Λ- or V-configurations shown in Fig. 1.6 where the arrows represent allowed spontaneous and stimulated transitions. In this experiment, crossover resonances arise from multiple upper levels and so we will illustrate with the V-system. Having two excited energy levels 1 and 2, the resonance frequencies to the ground state 0 are ν_1 and ν_2, which are assumed to be spaced less than a Doppler width.

Without the pump beam, each excited state would absorb with a Doppler-broadened profile and the net absorption would be the sum of two Gaussian profiles, one centered at ν_1 and one centered at ν_2. If the separation $|\nu_1 - \nu_2|$ is small compared to the Doppler width, they would appear as a single broadened absorption profile.

When the pump beam is turned on, two holes are burned in the ground state velocity distribution at velocities that put the atoms in resonance with ν_1 and ν_2. These two velocities would depend on the laser frequency ν. For example, at $\nu = \nu_1$, the probe absorption involving upper state 1 is from zero velocity atoms while the probe absorption involving the higher-energy state 2 arises from some non-zero, negative velocity atoms. At this frequency, the

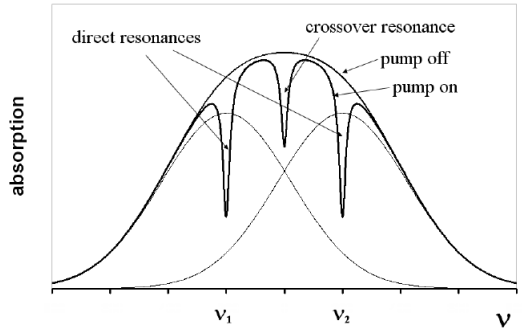

Figure 1.7: Absorption coefficient vs. the laser frequency for a V-type three-level atom. The three Bell shaped curves are with the pump off and give the Doppler-broadened absorption from the individual resonances at ν_1 and ν_2 and their sum. The pump on curve shows normal saturated absorption dips at $\nu = \nu_1$ and $\nu = \nu_2$ and a crossover resonance midway between.

pump beam burns one hole in the ground state for zero velocity atoms due to upper state 1 and another hole for some non-zero, positive-velocity atoms due to upper state 2. As with the two-level system, the hole at $v \approx 0$ leads to a decreased absorption to upper state 1 and produces a saturated absorption dip at $\nu = \nu_1$. A similar argument predicts a saturated absorption dip at $\nu = \nu_2$. Thus at $\nu = \nu_1$ and at $\nu = \nu_2$ there will be saturated absorption dips similar to those occurring in two-level atoms.

A third dip, the crossover resonance, arises at a frequency midway between at

$$\nu_{12} = (\nu_1 + \nu_2)/2 \tag{1.23}$$

All three dips are illustrated in Fig. 1.7 assuming $I/I_{sat} = 10$ and assuming that the excited levels have the same spontaneous transition rate γ and the same stimulated rate constant α_0.

At the crossover frequency, the pump and probe beams are resonant with the same two opposite velocity groups:

$$v = \pm c(\nu_2 - \nu_1)/2\nu_{12}. \tag{1.24}$$

Atoms at one of these two velocities will be resonant with one excited state and atoms at the opposite velocity will be resonant with the other excited state. The pump beam burns a hole in the ground state populations at both velocities and these holes affect the absorption of the probe beam, which is simultaneously also arising from atoms with these two velocities.

1.6 Energy levels of Rubidium

The rubidium atom has atomic number 37. In its ground state configuration it has one electron outside an inert gas (Argon) core and is described with the notation [Ar]5s. The Rb ground state configuration is said to have filled shells up to the 4p orbitals and a single valence electron in a 5s orbital. The next higher energy configuration has the 5s valence electron promoted to a 5p orbital with no change to the description of the remaining 36 electrons.

1.6.1 Fine structure levels

Within a configuration, there can be several fine structure energy levels differing in the energy associated with the coulomb and spin-orbit interactions. The coulomb interaction is associated with the normal electrostatic potential energy $kq_1q_2 = r_{12}$ between each pair of electrons and between each electron and the nucleus. The spin-orbit interaction is associated with the orientation energy $-\vec{\mu}\vec{B}$ of the magnetic dipole moment $-\vec{\mu}$ of each electron in the internal magnetic field $\vec{B}$ of the atom. The form and strength of these two interactions in rubidium are such that the energy levels are most accurately described in the L-S or Russell-Saunders coupling scheme. L-S coupling introduces new angular momentum quantum numbers L, S, and J. L is the quantum number describing the magnitude of the total orbital angular momentum $\vec{L}$ and similarly S is the quantum number describing the magnitude of the total electronic spin angular momentum $\vec{S}$. J is the quantum number describing the magnitude of the total electronic angular momentum $\vec{J}$, which is the sum of the total orbital and total spin angular momentum and in the L-S coupling regime can be expressed as:

$$\vec{J} = \vec{L} + \vec{S} \tag{1.25}$$

The values for L and S and J are specified in a notation ${}^{(2S+1)}L_J$ invented by early spectroscopists. The letters S, P, and D are used for L and correspond to $L = 0$, 1, and 2, respectively. The value of (2S + 1) is called the multiplicity and is thus 1 for S = 0 and called a singlet, 2 for S = 1/2 (doublet), 3 for S = 1 (triplet), etc. The value of J is annotated as a subscript to the value of L.

The sum of $\vec{\ell_i}$ or $\vec{s_i}$ over all electrons in any filled orbital is always zero. Thus for Rb configurations with only one valence electron, there is only one allowed value for L and S: just the value of ℓ_i and s_i for that electron. In its ground state (5s) configuration, Rb is described by $L = 0$ and $S = 1/2$. The only possible value for J is then 1/2 and the fine structure state would be labeled ${}^2S_{1/2}$. Its next higher (5p) configuration is described by $L = 1$ and

$S = 1/2$. In this configuration there are two allowed values $J = 1/2$ and $3/2$ and these two fine structure states are labeled $^2P_{1/2}$ and $^2P_{3/2}$.

1.6.2 Hyperfine structure levels

Within each fine structure level there can be an even finer set of hyperfine levels differing in the orientation energy associated with the nuclear magnetic moment in the magnetic field of the atom. The nuclear magnetic moment is much smaller than the electron magnetic moment and this is why the hyperfine splittings are so small. The nuclear magnetic moment is proportional to the spin angular momentum $\vec{I}$ of the nucleus, whose magnitude is described by the quantum number I. Allowed values for I depend on nuclear structure and vary with the isotope.

The hyperfine energy levels depend on the the total angular momentum $\vec{F}$ of the atom: the sum of the total electron angular momentum $\vec{J}$ and the nuclear spin angular momentum $\vec{I}$:

$$\vec{F} = \vec{I} + \vec{J} \tag{1.26}$$

The magnitude of $\vec{F}$ is characterized by the quantum number F with allowed values from $|J - I|$ to $|J + I|$. Each state with a different value of F will have a slightly different energy due to the interaction of the nuclear magnetic moment and the internal field of the atom. There is no special notation for labeling hyperfine states and F is usually written explicitly in energy level diagrams.

There are two naturally occurring isotopes of Rb: 72% abundant ^{85}Rb with $I = 5/2$ and 28% abundant ^{87}Rb with $I = 3/2$. For both isotopes, this leads to two hyperfine levels within the $^2S_{1/2}$ and $^2P_{1/2}$ fine structure levels ($F = I - 1/2$ and $F = I + 1/2$) and four hyperfine levels within the $^2P_{3/2}$ fine structure level ($F = I - 3/2$, $F = I - 1/2$, $F = I + 1/2$ and $F = I + 3/2$).

In Fig. 1.9 and 1.10 you can observe the theoretical D2 hyperfine energy level structure for both isotopes, while Fig. 1.8 shows an experimentally measured hyperfine structure spectrum.

1.6.3 Allowed transitions

The $^2S_{1/2}$ to $^2P_{1/2}$ transitions are all around 795 nm, while the $^2S_{1/2}$ to $^2P_{3/2}$ transitions are all around 780 nm. We will only discuss the 780 nm transitions that can be reached with the laser used in this experiment. Dipole transitions follow the selection rule $\Delta F = 0, \pm 1$. Thus, in each isotope, the allowed transitions from the $^2S_{1/2}$ to $^2P_{3/2}$ fall into two groups of three.

Because the hyperfine splitting between the two $^2S_{1/2}$ levels is large compared to the hyperfine splittings among the four $^2P_{3/2}$ levels, the groups will be well separated from each other. Within each group, the three probable transitions can be labeled by the F' of the $^2P_{3/2}$ state. These three transitions will be more closely spaced in energy.

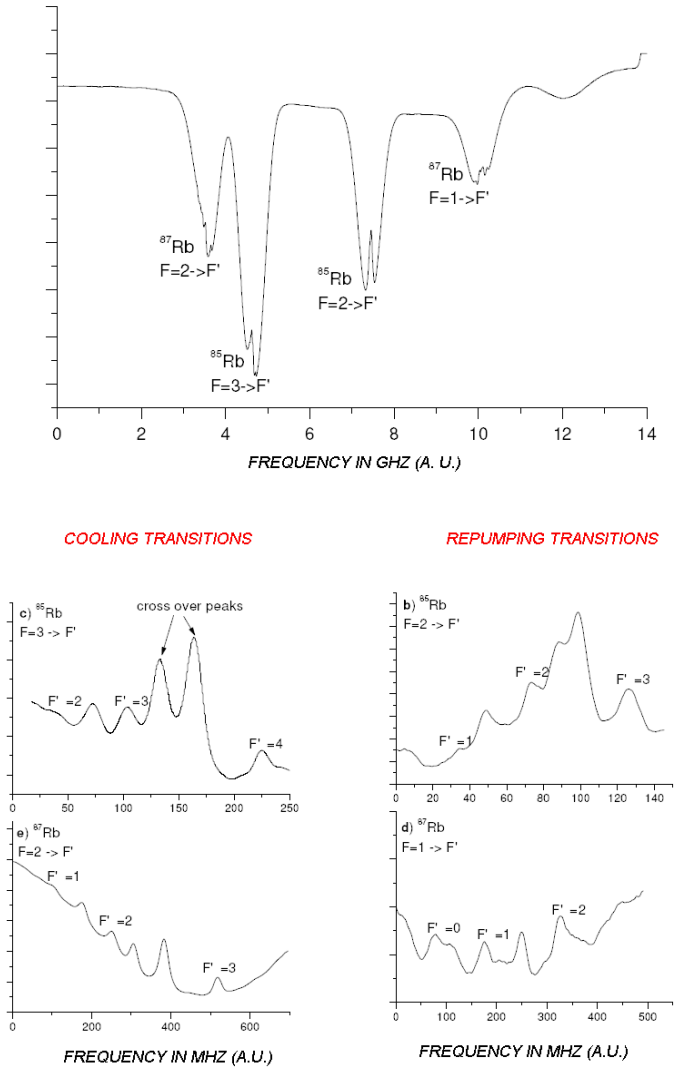

Figure 1.8: Measured spectra with cross over resonances of both rubidium isotopes.

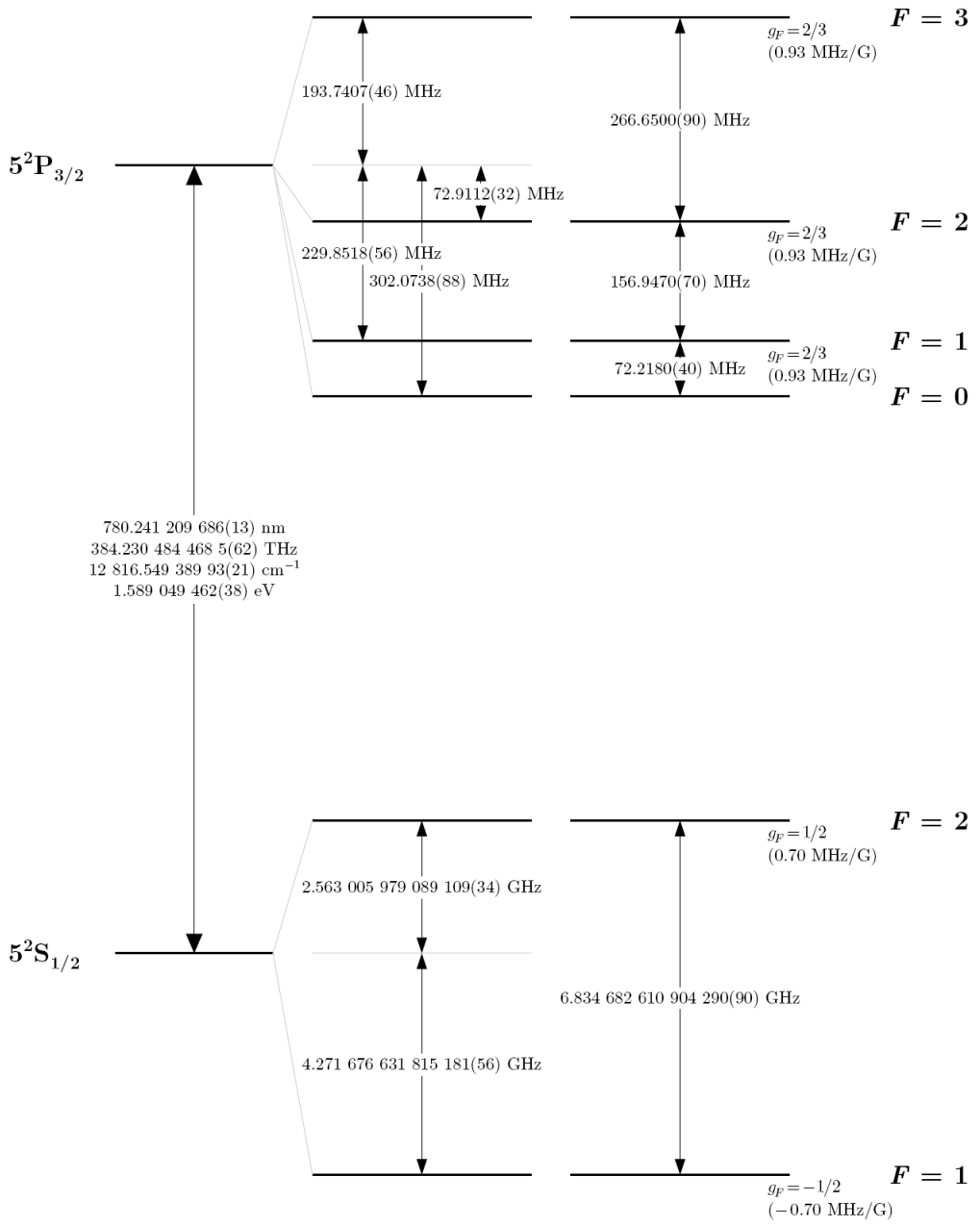

Figure 1.9: Rubidium 87 D2 transition hyperfine structure, with frequency splittings between the hyperfine energy levels.

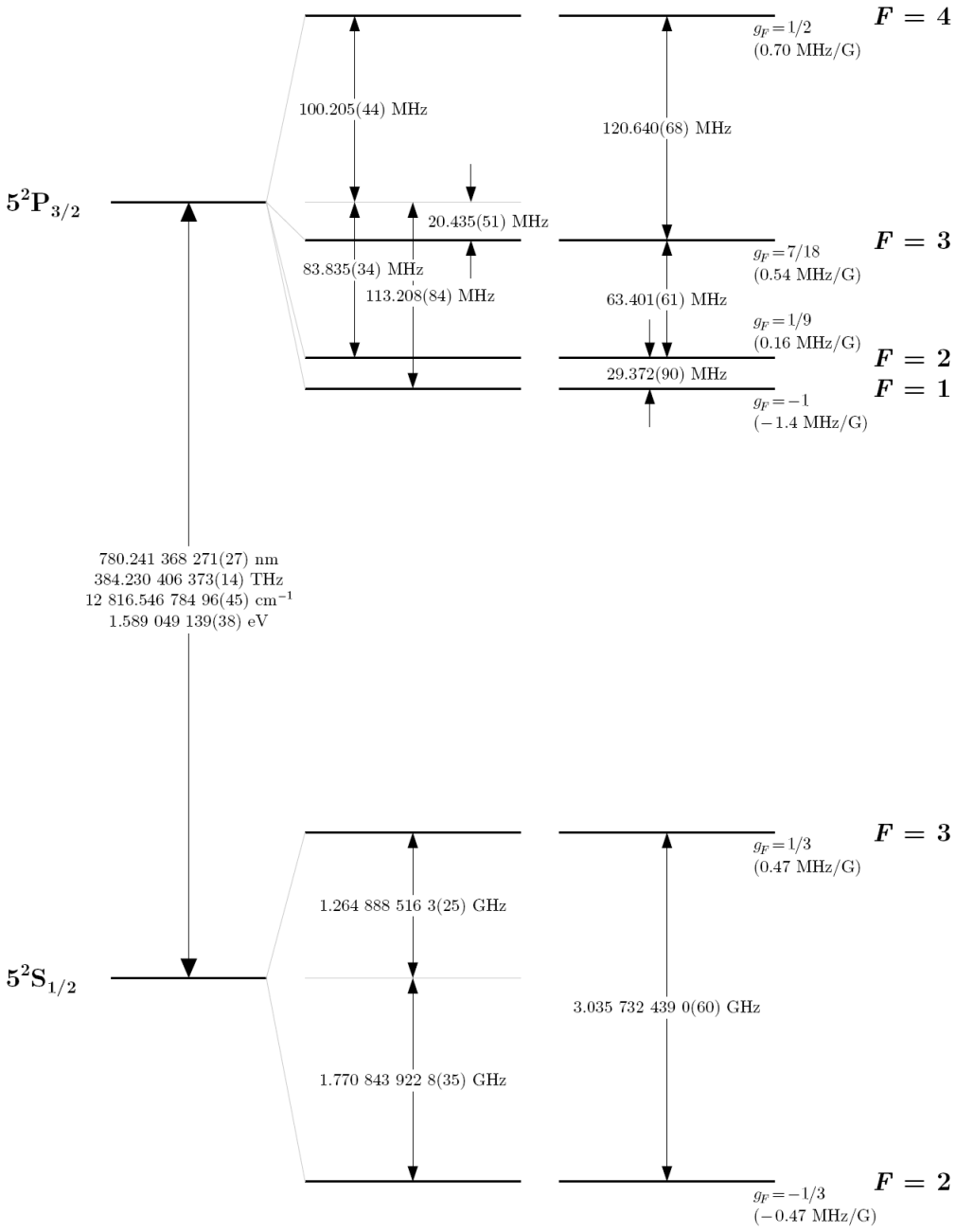

Figure 1.10: Rubidium 85 D2 transition hyperfine structure, with frequency splittings between the hyperfine energy levels.

1.7 Frequency modulation (FM) spectroscopy

Frequency modulation spectroscopy is a very sensitive spectroscopy method. It produces a signal which is proportional to the derivative of the atomic resonances. In the spectroscopy part of this student experiment, FM-spectroscopy method will be used to measure the frequency of the Lamb-dips and the crossovers. For the MOT-part of the experiment, the FM-spectroscopy signal will be also used to create the error-signal for the laser stabilization (§ 3.2).

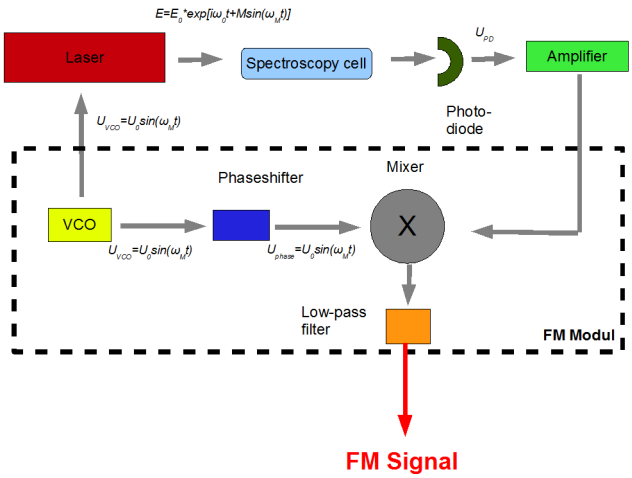

Figure 1.11: Principle of FM-spectroscopy.

This method is schematically illustrated in Fig. 1.11. The current of the laser is modulated by a small modulation at a fixed frequency ω_{M} which is produced by a VCO (voltage controlled oscillator).

The electrical field of the wave emitted from the diode laser is in this case

$$E(t) = E_0 \times e^{i[\omega_0 t + M sin(\omega_M t)]} + c.c. \tag{1.27}$$

where ω_0 is the optical frequency, E_0 the amplitude of the light wave and M is the modulation index. For small modulation indexes ($M << 1$) one can make the following approximation:

$$\begin{aligned} E(t) &= E_0 \times e^{i[\omega_0 t]} e^{[iM sin(\omega_M t)]} + c.c. \\ &\approx E_0 \times e^{i[\omega_0 t]} [1 + iM sin(\omega_M t)] + c.c. \\ &= E_0 \times e^{i[\omega_0 t]} [1 - \frac{M}{2} e^{-i[\omega_M t]} + \frac{M}{2} e^{+i[\omega_M t]}] + c.c \\ &= E_0 \times [e^{i[\omega_0 t]} - \frac{M}{2} e^{i[(\omega_0 - \omega_M) t]} + \frac{M}{2} e^{i[(\omega_0 + \omega_M) t]}] + c.c \end{aligned} \tag{1.28}$$

Hence the emitted laser frequencies now consist of a strong carrier with a frequency ω_0 and two weak sidebands at frequencies $\omega_0 \pm \omega_M$. If the modulated beam is sent through the vapor cell, the atoms absorb a part of the beam when the frequency is on resonance with one of the atomic transitions. The carrier frequency and the sideband frequencies have different transmission strengths if they are close to an atomic transition or not. Due to dispersion (the frequency-dependence of the index of refraction) the different components also have a "individual" phase-shift after the transmission through the vapor cell.

The electric field of the transmitted wave has now the following form:

$$\begin{aligned} E(t)_{\text{trans}} = E_0 \times [T_0 e^{-i\phi_0} e^{i[\omega_0 t]} - \frac{M}{2} T_- e^{-i\phi_-} e^{i[(\omega_0-\omega_M)t]} \\ + \frac{M}{2} T_+ e^{-i\phi_+} e^{i[(\omega_0+\omega_M)t]}] + c.c, \end{aligned} \tag{1.29}$$

where $T_j = e^{-\rho_j} (j = 0, -, +)$ are the transmission coefficients with the frequency depending dampings $\rho_j = \rho_j(\omega)$ and $\phi_j = \phi_j(\omega)$ the frequency dependent phase shifts of the different frequency components (ω_0,$\omega_0-\omega_M$,$\omega_0+\omega_M$).

The intensity of the transmitted (averaged) signal is measured with a fast photodiode and this device outputs a voltage $U_{\text{PD}} \propto < I(t) > = < \frac{c}{8\pi}|E(t)|^2 >$. Due to $M \ll 1$ terms with M^2 can be neglected. All terms with $sin(2\omega_0 t)$ or $cos(2\omega_0 t)$ also cancel because the photodiode is averaging over fast oscillations which are usually out of its bandwidth. We can further assume that $|\rho_0 - \rho_\pm| \ll 1$ and $|\phi_0 - \phi_\pm| \ll 1$.

With these approximations the intensity at the photodiode (with the absorption difference $\Delta T = T_+ - T_-$ and relative phase shift difference $\Delta\Phi = \Phi_+ - \Phi_-$) can be written as

$$\begin{aligned} < I(t) > \propto 2T_0^2 - MT_0T_-(e^{i[\phi_- - \phi_0]} e^{i[\omega_M)t]} + e^{-i[\phi_- - \phi_0]} e^{-i[\omega_M)t]}) \\ + MT_0T_+(e^{i[\phi_0 - \phi_+]} e^{i[\omega_M)t]} + e^{-i[\phi_0 - \phi_+]} e^{-i[\omega_M)t]}) \end{aligned} \tag{1.30}$$

A Taylor expansion of $e^{i[\phi_0 - \phi_\pm]}$ leads to

$$\begin{aligned} < I(t) > \; &\propto \; T_0^2 - MT_0\Delta T cos(\omega_M t) - MT_0 sin(\omega_M t)[T_-(\phi_0 - \phi_-) + T_+(\phi_0 - \phi_+)] \\ &\approx \; T_0^2 - MT_0\Delta T cos(\omega_M t) - MT_0 sin(\omega_M t)[T_0(\phi_0 - \phi_-) + T_0(\phi_0 - \phi_+)] \\ &= \; T_0^2 - MT_0\Delta T cos(\omega_M t) - MT_0 sin(\omega_M t)\Delta\phi \end{aligned} \tag{1.31}$$

In order to filter the $sin(\omega_m t)$ and the $cos(\omega_m t)$ dependence, the signal from the photodiode is demodulated by a mixer. The mixer multiplies the signal from the VCO with the amplified signal from the photodiode. The signal from the VCO is additional shifted by a phase ϕ to maximize the phase

matching between the two signals. The signal after the mixer is then given (T_0^2 leads only to a constant offset) by:

$$\begin{aligned} U_{\text{mixer}}(t) &\propto U_{\text{PD}}(t) \cdot U_{\text{VCO}}(t) \\ &\propto [MT_0\Delta T_- cos(\omega_M t) - MT_0 sin(\omega_M t)\Delta\phi] cos(\omega_M t + \varphi) \\ &= M\{\frac{\Delta T}{2}[cos(\varphi) + cos(2\omega_M t + \varphi)] - \frac{\Delta\phi}{2}[sin(\varphi) + sin(2\omega_M t + \varphi)]\} \end{aligned} \tag{1.32}$$

The fast oscillating $2\omega t$ parts can be suppressed by a low-pass filter and one gets the final signal (see also Fig. 1.12):

$$U_{\text{FM}} \propto \frac{\Delta T}{2} cos\varphi - \frac{\Delta\Phi}{2} sin\varphi \tag{1.33}$$

The final signal doesn't depend on the time and by changing the phase shift it is possible to switch between the cos - and the sin- term.

By applying a Taylor expansion on ΔT one can show that the cos-term is proportional to the derivative of the atomic resonance (Fig. 1.13):

$$\begin{aligned} \Delta T &= T_+ - T_- \\ &= T(\omega_0 + \omega_M) - T(\omega_0 - \omega_M) \\ &\approx T(\omega_0) + \frac{dT}{d\omega}|_{\omega_0}\omega_M + \frac{1}{2}\frac{d^2T}{d\omega^2}|_{\omega_0}\omega_M^2 - T(\omega_0) + \frac{dT}{d\omega}|_{\omega_0}\omega_M - \frac{1}{2}\frac{d^2T}{d\omega^2}|_{\omega_0}\omega_M^2 \\ &= \frac{dT}{d\omega}|_{\omega_0} 2\omega_M \end{aligned} \tag{1.34}$$

The positions of atomic resonances can be easily identified by the points where the FM-signal is crossing zero.

At the student's lab the mixing frequency and the demodulation of the signal is done in the FM modulation boxes, built from the electronics workshop of the Physical Institute. The mixing frequency is about 21MHz and the modulation index and the phase shift are fixed and should not be changed!

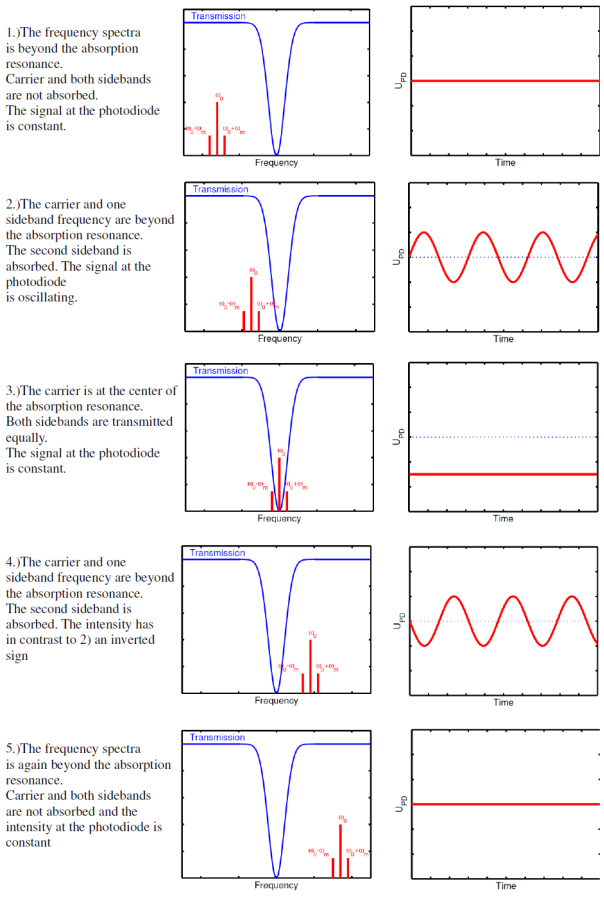

Figure 1.12: Signal behavior of a modulated laser beam at a resonance on a photodiode.

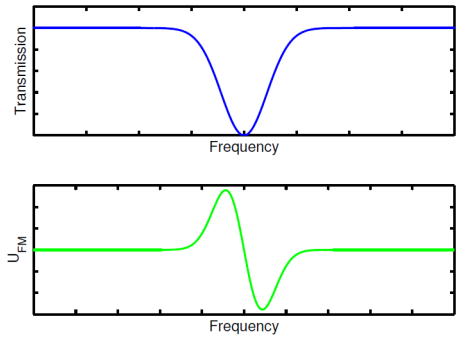

Figure 1.13: At a certain phase shift, the FM signal is proportional to the derivative of an atomic resonance.

Chapter 2

Magneto-Optical Trap

The combination of laser cooling and atom trapping has produced astounding new tools for atomic physicists. These experiments require the exchange of momentum between atoms and an optical field, usually at frequencies nearly resonant to an atomic transition. The energy of the light $\hbar\omega$ changes the internal energy of the atom, and the angular momentum $\hbar k$ changes the orbital angular momentum l, of the atom, as described by the well-known selection rule $\Delta l = \pm 1$. In contrast, the linear momentum of the light $p = \hbar k$ cannot change the internal atomic degrees of freedom and therefore must change the momentum of the atoms in the laboratory frame. The force resulting from this momentum exchange between the light field and the atoms can be used in many ways to control atomic motion and is the subject of this theory section.

If the light is absorbed, the atom makes a transition to an excited state, and the return to the ground state can be either by spontaneous or by stimulated emission. The nature of the optical force that arises from these two processes is quite different and will be described separately.

2.1 Radiative Optical Forces

In the simplest case the momentum exchange between a monochromatic light field and the atoms results in a force

$$\overrightarrow{F} = \frac{d\overrightarrow{p}}{dt} = \hbar\overrightarrow{k}\gamma_p \tag{2.1}$$

where γ_p is the excitation rate of the atoms. The absorption leaves the atoms in their excited state and then, if the light intensity is low enough, they are much more likely to return to the ground state by spontaneous emission

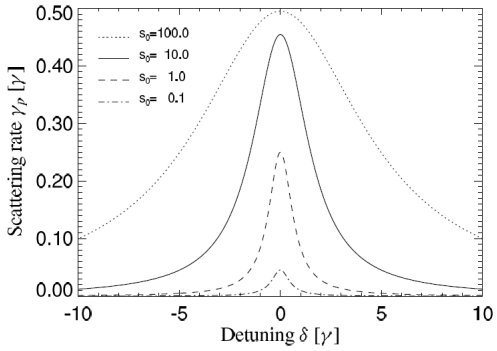

Figure 2.1: Scattering rate γ_p as a function of the detuning δ for several values of the saturation parameter s0. Note that for s0 $>$ 1 the line profiles start to broaden substantially due to power broadening.(Taken from [1])

than by stimulated emission. In this case the resulting emitted light carries off a momentum $\hbar\overrightarrow{k}$ in a random direction. In first approximation, the momentum exchange from the spontaneous emission averages to zero, so that the net total force is given by the above equation.

The scattering rate γ_p depends on the laser detuning from the atomic resonance $\delta = \omega_l - \omega_a$, where ω_l is the laser frequency and ω_a is the atomic resonance frequency (2.1)). This detuning is measured in the atomic reference frame, and to calculate the absorption and scattering rate it is necessary to consider the Doppler-shifted laser frequency in the moving atom's reference frame.

The excitation rate γ_p for a two-level atom is given by a Lorentzian

$$\gamma_P = \frac{s_0\gamma/2}{1 + s_0 + [2(\delta + \omega_D)/\gamma]^2} \tag{2.2}$$

where $\gamma = 1/\tau$ is an angular frequency corresponding to the decay rate of the excited state. Here $s_0 = I/I_S$ is the ratio of the light intensity I to the so-called saturation intensity

$$I_s = \frac{\pi hc}{3\lambda^3\tau} \tag{2.3}$$

where $\gamma_P(I_s) = \frac{1}{2}\gamma_P(\infty)$. I_s is a few mW/cm^2 for typical atomic transitions.

The Doppler shift seen by the moving atoms is

$$\omega_D = -\overrightarrow{k}\overrightarrow{v} \tag{2.4}$$

(note that $\overrightarrow{k}$ opposite to $\overrightarrow{v}$ produces a positive Doppler shift). The force is thus velocity dependent and this fact is exploited in laser cooling.

The maximum attainable deceleration is obtained for very high light intensities. High-intensity light can produce faster absorption, but it also causes equally fast stimulated emission; the combination produces neither deceleration nor cooling. The momentum transfer to the atom in stimulated emission is in the opposite direction to what it was in absorption, resulting in a net transfer of zero momentum. Since high intensity causes the atom to divide its time equally between ground and excited states, the force is limited to

$$\overrightarrow{F} = \hbar \overrightarrow{k} \gamma_p \tag{2.5}$$

so the deceleration saturates at a value

$$a_{max} = \frac{\hbar \overrightarrow{k} \gamma}{2M} \tag{2.6}$$

2.2 Optical molasses

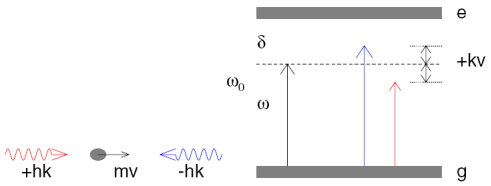

Figure 2.2: Standard configuration for laser cooling in an optical molasses. By detuning the laser frequency ω below the resonance frequency ω_0 the frequency of the laser opposing the atomic motion is shifted toward resonance, whereas the frequency of the other laser beam is shifted out of resonance.(Taken from [1])

Using Eq. 2.2 it is straightforward to calculate the radiative force on atoms moving in a standing wave produced by two counter-propagating laser beams. In the low-intensity case, where stimulated emission is not important, the forces from the two light beams are simply added to give

$$\overrightarrow{F}_{OM} = \overrightarrow{F}_{+} + \overrightarrow{F}_{-} \tag{2.7}$$

where $\overrightarrow{F}_{\pm}$ are found from Eqs. 2.1 and 2.2. Then the sum of the two forces is

$$\overrightarrow{F}_{OM} \cong \frac{8\hbar k^2 \delta s_0}{\gamma[1 + s_0 + (2\delta/\gamma)^2]^2} \overrightarrow{v} \equiv -\beta \overrightarrow{v} \propto -\overrightarrow{v} \tag{2.8}$$

where terms of order $(kv/\gamma)^4$ and higher have been neglected. For small enough velocities, the slowing force is proportional to the velocity. This results in viscous damping [5] and gives this technique the name **Optical Molasses (OM)** [6]. The resulting forces are plotted in Fig. 2.3. For $\delta < 0$, the sum of the forces opposes the velocity and therefore viscously damps the atomic motion. The force $\overrightarrow{F}_{OM}$ has maxima near

$$v \approx \pm \frac{\gamma\sqrt{s_0 + 1}}{2k} \tag{2.9}$$

and decreases rapidly for larger velocities.

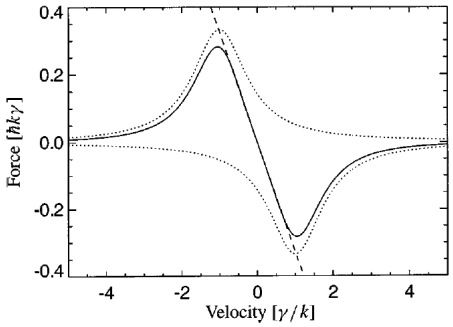

Figure 2.3: Velocity dependence of the optical damping forces for 1D optical molasses. The two dotted traces show the force from each beam, and the solid curve is their sum. The straight line shows how this force mimics a pure damping force over a restricted velocity range. These are calculated for $s_0 = 2$ and $\delta = -\gamma$, so there is some power broadening evident. (Taken from [4])

2.2.1 Temperature in laser cooling

If there was no other influence on the atomic motion, all atoms would quickly decelerate to $v = 0$, and the sample would reach $T = 0$, a clearly non-physical result. In fact there are two limits to the obtainable temperature: the first one is related to the absorption or emission of a single photon and it is called **recoil limit** while the second one is related to a statistical effect from spontaneous emission, which gives rise to a heating process and leads to the **doppler temperature limit**. Let's see them more in detail.

In the elementary absorption or emission process of a single photon, the atoms obtain a minimum recoil velocity $v_r = \frac{\hbar k}{M}$ and the corresponding energy

change can be related to a temperature, the recoil temperature, defined as

$$k_B T_r \equiv \frac{\hbar^2 k^2}{M} \tag{2.10}$$

This limit is generally regarded as the lower limit for optical cooling processes (although there are a few clever schemes that can cool below it) and for most atomic species is on the order of few hundreds of μK.

The other limiting temperature, called doppler temperature, is usually higher than the recoil one and it is due to the fact that as the atoms absorb photons and spontaneously emit them in random directions they will not only have momentum no smaller than that of a laser photon, but they must also scatter one photon momentum in a random direction every natural lifetime of the excited state. If this lifetime is short then the random walk in momentum space (also called brownian motion) occurs at a rate too fast to remain near the origin, leading to an effective heating due to spontaneous emission. You can find an appropriate theoretical treatment of this process in [4], while here we will give a more euristic explanation.

At each emission or absorption, the atom momentum is changed by a discrete size steps $\hbar k$, leading to an average kinetic energy change by at least the recoil energy

$$E_r = \frac{\hbar^2 k^2}{2M} = \hbar\omega_r \tag{2.11}$$

This means that the average frequency of each absorption is $\omega_{abs} = \omega_a + \omega_r$, and the average frequency of each emission is $\omega_{emit} = \omega_a - \omega_r$. Thus the light field loses an average energy of

$$\hbar\left(\omega_{abs} - \omega_{emit}\right) = 2\hbar\omega_r \tag{2.12}$$

for each scattering. This loss occurs at a rate $2\gamma_p$ (two beams), and the energy is converted to atomic kinetic energy because the atoms recoil from each event. Since these recoils are in random directions the atomic sample is thereby heated.

The competition between this heating with the damping force of Eq. 2.8 results in a non-zero kinetic energy and gives rise to a steady state, where the rates of heating and cooling are equal. Equating the cooling rate, $\overrightarrow{F}_{OM} \cdot \overrightarrow{v}$, to the heating rate, $4\hbar\omega_r\gamma_p$, delivers the steady-state kinetic energy is

$$E_{kin} = \frac{\hbar\gamma}{8}\left(\frac{2|\delta|}{\gamma} + \frac{\gamma}{2|\delta|}\right) \tag{2.13}$$

This result is dependent on the laser detuning $|\delta|$, and it has a minimum at $2|\delta|/\gamma = 1$, i.e. $\delta = -\gamma/2$. The temperature found from the kinetic energy

is then

$$T_D = \frac{\hbar\gamma}{2k_B} \tag{2.14}$$

where k_B is Boltzmann's constant and T_D is called the **Doppler temperature** or the Doppler cooling limit. For ordinary atomic transitions, T_D is typically below 1 mK. This remarkable result predicts that the final temperature of atoms in optical molasses is independent of the optical wavelength, atomic mass, and laser intensity (as long as it is not too large).

2.3 Magneto-Optical Trap

The most widely used trap for neutral atoms is a hybrid trap called **magneto-optical trap (MOT)** because it employs both optical and magnetic fields. It was first demonstrated in 1987 [7] and its operation depends on both inhomogeneous magnetic fields and radiative selection rules to exploit both optical pumping and the strong radiative force. The radiative interaction provides the cooling that helps in loading the trap, while the inhomogeneous magnetic field exerts a recalling force towards the center of the field, allowing a stable trapping.

The MOT is a robust trap, which does not critically depend on precise balancing of the counter-propagating laser beams or on a very high degree of polarization. The magnetic field gradients are of the order of $10G/cm = 10^{-3}T/cm$ and can readily be achieved with simple coils. The trap can be operated inside a vacuum chamber in which alkali atoms, in our case ^{85}Rb atoms are captured from a background vapor ejected by so called dispensers. Furthermore, low-cost - in our case homebuilt - diode lasers are used to produce the light appropriate for all the alkali (except Na), so the MOT has become an inexpensive ways to produce atomic samples with temperatures below 1 mK.

Trapping in a MOT works by optical pumping of slowly moving atoms in a linearly inhomogeneous magnetic field $B = B(z) = Az$. This quadrupole field is created by a pair coils powered by counter circulating currents, so called Anti-Helmholtz coils. Atomic transitions with the simple scheme of $J_g = 0 \rightarrow J_e = 1$ have three Zeeman components in a magnetic field, each excited by a different polarization $\pi, \sigma^{\pm}$, whose frequencies tune with field (and therefore with position) as shown in Fig. 2.4 for 1D.

Two counter propagating laser beams of opposite circular polarization, each detuned below the zero field atomic resonance by δ, are incident as shown in Fig. 2.4. Because of the Zeeman shift, the excited state $M_e = +1$ is shifted up for $B > 0$, whereas the state with $M_e = -1$ is shifted down.

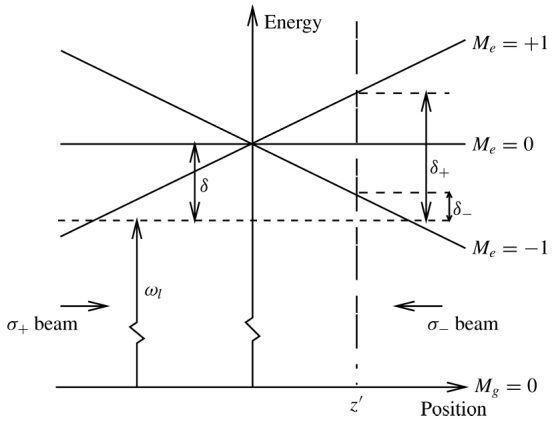

Figure 2.4: Arrangement for a MOT in 1D. The horizontal dashed line represents the laser frequency seen by atoms at rest in the center of the trap. Because of the Zeeman shifts of the atomic transition frequencies in the inhomogeneous magnetic field, atoms at $z = z_0$ are closer to resonance with the σ^- laser beam than with the σ^+ beam, and are therefore driven toward the center of the trap. (Taken from [4])

At position z the magnetic field therefore tunes the $\Delta M = -1$ transition closer to resonance and the $\Delta M = +1$ transition further outfrom resonance. If the polarization of the laser beam incident from the right is chosen to be σ^- and correspondingly σ^+ for the other beam, more photons are scattered from the σ^- beam than from the σ^+ beam. Thus the atoms are driven toward the center of the trap where the magnetic field is zero. On the other side of the center of the trap, the roles of the $M_e = \pm 1$ states are reversed and now more light is scattered from the σ^+ beam, again driving the atoms towards the center. The situation is analogous to the velocity damping in an optical molasses from the Doppler effect as discussed above, but here the effect operates in position space, whereas for molasses it operates in velocity space. Since the laser light is detuned below the atomic resonance in both cases, compression and cooling of the atoms is obtained simultaneously in a MOT.

So far the discussion has been limited to the motion of atoms in 1D. However, the MOT scheme can easily be extended to 3D by using six instead of two laser beams (Fig. 2.5). Furthermore, even though very few atomic species have transitions as simple as $J_g = 0 \rightarrow J_e = 1$, the scheme works for any $J_g \rightarrow J_e = J_g + 1$ transition. Atoms that scatter mainly from the σ^+ laser beam will be optically pumped toward the $M_g = +J_g$ substate, which

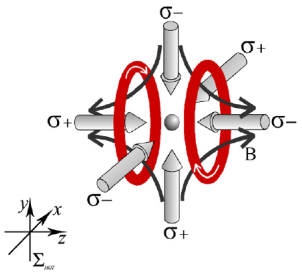

Figure 2.5: Three pairs of counter propagating laser beams as well as a pair of Anti-Helmholtz coils provide the necessary ingredients for a Magneto-Optical Trap.

forms a closed system with the $M_e = +J_e$ substate.

For a description of the motion of the atoms in a MOT, consider the radiative force in the low-intensity limit (see Eqs. 2.1 and 2.2). The total force on the atoms is given by

$$\overrightarrow{F}_{OM} = \overrightarrow{F}_{+} + \overrightarrow{F}_{-} \tag{2.15}$$

where $\overrightarrow{F}_{\pm}$ are found from Eqs. 2.1 and 2.2, and the detuning $\delta_{\pm}$ from the atomic resonance

$$\delta_{\pm} = \delta \mp \overrightarrow{k} \cdot \overrightarrow{v} \pm \frac{\mu' B}{\hbar} \tag{2.16}$$

Here $\mu' \equiv (g_e M_e - g_g M_g)\,\mu_B$ is the effective magnetic moment for the transition used. Note that the Doppler shift $\omega_D = -\overrightarrow{k} \cdot \overrightarrow{v}$ and the Zeeman shift $\omega_Z = \mu' B/\hbar$ both have opposite signs for opposite beams.

When both the Doppler and Zeeman shifts are small compared with the detuning δ, the denominator of the force can be expanded as for relation 2.8 and the result becomes

$$\overrightarrow{F} = -\beta \overrightarrow{v} + \kappa \overrightarrow{r} \tag{2.17}$$

where the damping coefficient β is defined in relation (3). The spring constant κ arises from the similar dependence of $\overrightarrow{F}$ on the Doppler and Zeeman shifts and is given by

$$\kappa = \frac{\mu' \beta}{\hbar k} A \tag{2.18}$$

where A is the magnetic field gradient. The force of Eq. 2.17 leads to damped harmonic motion of the atoms, where the damping rate is given by $\Gamma_{MOT} = \beta/M$ and the oscillation frequency by $\omega_{MOT} = \sqrt{\kappa/M}$. For magnetic field gradients $A \approx 10 G/cm$, the oscillation frequency is typically a few kilohertz, and this is much smaller than the damping rate that is

typically a few hundred kilohertz. Thus the motion is over-damped, with a characteristic restoring time to the center of the trap of $2\Gamma_{MOT}/\omega_{MOT}^2$, which is of the order of several milliseconds for typical values of the detuning and intensity of the lasers.

So far, we have considered a two level system, but real atoms have a much more complicated level structure. Which transition to choose for the MOT laser cooling? A first guess would be to select the transition that has the highest excitation rate, leading to the maximum absorption and cooling, but, for any multilevel system, a very important requirement for an efficient MOT is to operate between atomic transitions which form a closed system to avoid losses from the cooling cycle. If the chosen excited level has more than one decay channel, then the most frequent ones have to be addressed by additional laser beams to repump the atoms into the levels used for the cooling transition, thus forming a maximally closed loop of transitions.

2.4 Comparison of relevant temperature scales in laser cooling

It is convenient to use the label of temperature to describe an atomic sample whose average kinetic energy $\langle E_k \rangle$ in one dimension has been reduced by the laser light, and this is written simply as

$$\langle E_k \rangle = \frac{1}{2} k_B T \tag{2.19}$$

where k_B is Boltzmann's constant.

The first characteristic temperature corresponds to the energy associated with atoms whose speed and concomitant Doppler shift puts them just at the boundary of absorption of light. This defines the highest velocity class of atoms that can be efficiently cooled and trapped by a MOT, while the atoms that have higher initial velocities can escape from the trap. So the **capture velocity** is defined as $v_c \equiv \frac{\gamma}{k} \approx 1m/s$, and the corresponding temperature is

$$k_B T_C \equiv \frac{M\gamma^2}{k^2} \tag{2.20}$$

and is typically several mK (for $^{85}Rb, T_C = 222.12mK$).

The next characteristic temperature is the **Doppler temperature** and it is related to the energy associated with the natural width of atomic transitions. It is given by

$$k_B T_D \equiv \frac{\hbar\gamma}{2} \tag{2.21}$$

Because it corresponds to the limit of certain laser cooling processes, it is often called the Doppler limit, and is typically several hundred μK (for ${}^{85}Rb, T_D = 143.41\mu K$). Associated with this temperature is the one-dimensional velocity $v_D = \sqrt{\frac{k_B T_D}{M}}$ (for ${}^{85}Rb, v_D = 11.85 cm/s$).

The last of these three characteristic temperatures is the **recoil temperature** corresponds to the energy associated with a single photon recoil that we defined as

$$k_B T_r \equiv \frac{\hbar^2 k^2}{M} \tag{2.22}$$

and is generally regarded as the lower limit for optical cooling processes (although there are a few clever schemes that can cool below it). It is typically a few μK, and corresponds to speeds of $v_r \approx 1 cm/s$ (for ${}^{85}Rb, v_r = 0.602 cm/s, T_r = 0.370\mu K$.

These three temperatures are related to one another through a single parameter ϵ that is ubiquitous in describing laser cooling. It corresponds to the ratio of the recoil frequency $\omega_r \approx \frac{\hbar k^2}{2M}$ to the natural width γ, and as such embodies most of the important information that characterize laser cooling on a particular atomic transition. Typically $\epsilon \approx 10^{-3} - 10^{-2}$, and is given by

$$\epsilon \equiv \omega_r / \gamma = \frac{\hbar k^2}{2M\gamma} \tag{2.23}$$

From this is clear that $T_r = 4\epsilon T_D = 4\epsilon^2 T_C$

2.5 Trap loading and loss processes

The time dependence of the atom number in the trap is given by an interplay of trap loading and different loss processes. As we will see at the end of this subsection, the time dependency of the atomic density can be described by a rate equation. First we will discuss the different terms:

2.5.1 Loading Rate

The atoms which we trap in our MOT are emitted from a so called dispenser, which is located in the vacuum system (§ 3.4). The dispenser produces a vapor with a certain partial pressure of Rb that is related to the current that runs through the dispenser, heating it. Atoms from the background vapor can be captured in the MOT when they loose their kinetic energy by scattering photons from the laser beams until they have nearly zero energy. Depending on the scattering rate and the beam diameters one

can define a capture velocity (the largest energy which is trappable), which is typically in the order of 10 m/s. This means that only a small fraction of the atoms from the vapor can be trapped in a MOT.

The change in the atom number can then be written as:

$$\frac{dN}{dt} = L(I_{\text{Dispenser}};\gamma_{\text{p}}) > 0 \tag{2.24}$$

where L is the loading rate, which itself is a function of the dispenser current $I_{\text{Dispenser}}$ and the scattering rate (§ 2.1) of the atoms γ_{p}. If there were no loss mechanisms in the sample, the atom number in the MOT would diverge to infinity!

2.5.2 One-body Losses

The trapped atoms in the MOT are lost via collisions. The most dominant loss mechanism for a MOT are collisions between a "hot" atom from the background gas and an atom from the MOT. The gain in kinetic energy is normally much larger as the capture velocity of the MOT and the particle leaves the trapping region. The rate for this process depends on the atom number in the trap and can be written as

$$\frac{dN}{dt} = -\alpha N \tag{2.25}$$

where α corresponds to the one-body loss coefficient.

2.6 Rate-Equation

The time-dependent change in the atom number can be written by combining the two differential equations for the loading and one-body loss processes:

$$\frac{dN}{dt} = L - \alpha N \tag{2.26}$$

During the preparation of the lab week, you have to solve this differential equation. What is the solution at the beginning of the loading process and what will be the steady state? What is the typical time scale ("loading time") for the loading process of a MOT?

For higher densities one also has to consider density dependent two-body collisions, i.e. fine structure changing collisions, where the fine structure of the atomic pair has changed after the collision and the loss in internal energy

leads to an increase of the kinetic energy larger than the capture velocity. This leads to a more complicated differential equation for the atom number:

$$\frac{dN}{dt} = L - \alpha N - \beta N^2 \tag{2.27}$$

with β being the two-body decay coefficient.

2.7 Temperature measurement via release and recapture

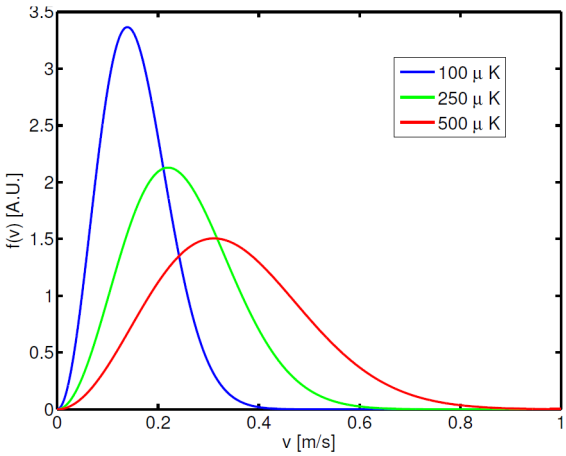

Figure 2.6: Velocity distribution for different temperatures in a MOT.

The temperature of a MOT can be measured by the "release and recapture" method, assuming that the velocity distribution of the atoms corresponds to a Maxwell -Boltzmann distribution. The size of the MOT is much smaller than the trapping volume, which is connected to the diameters of the laser beams. When the cooling beams of the MOT are switched off after loading, the atoms don't feel any trapping potential and they start to fly in the direction that is given by their velocity at the time when the MOT is switched off. Due to the low density of the MOT ($\approx 10^9 cm^{-3}$), the mean free path is large and collisions between the atoms can be neglected. After a certain time (typically several ms) the cooling beams are again switched on and the particles with low velocities are still within the crossing of the laser beams and thus are recaptured. Particles with higher velocities have already left the crossing of the beams and so they are not recaptured. When the

delay between switch-off and switch-on the MOT is increased, the amount of atoms recaptured in the MOT becomes smaller and smaller. At a fixed delay time, the amount of recaptured atoms is larger the lower the temperature of the sample is.

The amount of recaptured atoms at a certain time can be modeled in the following way. The velocity distribution of the atoms is given by a Maxwell-Boltzmann distribution $f(v)$ with

$$f(v) = \frac{4}{\sqrt{\pi}} \frac{v^2}{\alpha^3} e^{[-v^2/\alpha^2]} \tag{2.28}$$

with $\alpha = \sqrt{2k_BT/M}$. At $t = 0$, all atoms are assumed to be at the center of the trap i.e. $r = 0$. After an expansion time t, the velocity distribution is represented by a spatial distribution via $v = r/t$.

The spatial distribution at a time t is thus given by

$$f(r,t) = \frac{4}{\sqrt{\pi}} \frac{r^2}{t^2\alpha^3} e^{[-r^2/(\alpha^2 t^2)]} \tag{2.29}$$

The amount of atoms which are within a sphere with a radius R can be calculated by integrating over this sphere:

$$\frac{N(t)}{N(0)} = \int_{r \leq R} d^3 r f(r,t) \tag{2.30}$$

The analytical solution of this integral is:

$$\frac{N(t)}{N(0)} = erf(\chi) - \frac{2}{\sqrt{\pi}} \chi e^{-\chi^2} \tag{2.31}$$

where $\chi = \sqrt{\frac{M}{k_BT}} \frac{R}{t}$. The release and recapture measurement in the FP-lab can be done by switching off the MOT beams via a TTL signal that controls the power output of the AOM driver used to adjust the detuning of the cooling laser. The time delay can be changed by a delay box. The gradient fields for the MOT coils also have to be switched off during the measurement.

2.8 Links

An introduction into the field of laser-cooling with nice applets can be found at

- Homepage of Prof. Meschede at the University of Bonn
- University of Bouler / Colorado

Chapter 3

Experimental Setup

3.1 Laser Diodes

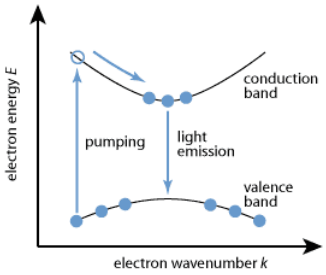

Figure 3.1: Physical origin of gain in a semiconductor.

Laser diodes (or diode lasers, unfortunately these names are synonyms) are electrically pumped semiconductor lasers in which the gain is generated by an electrical current flowing through a p–n junction. In such a heterostructure, electrons and holes can recombine, releasing the energy portions as photons. Semiconductor lasers are lasers based on semiconductor gain media, where optical gain is usually achieved by stimulated emission at an interband transition under conditions of a high carrier density in the conduction band. The physical origin of gain in a semiconductor is illustrated in Fig. 3.1. Without pumping, most of the electrons are in the valence band. A pump beam (or in our case an electrical pumping mechanism) with a photon energy slightly above the band gap energy can excite electrons into a higher state in the conduction band, from where they quickly decay to states near the bottom of the conduction band. At the same time, the holes generated in the valence band move to the top of the valence band. Electrons in the conduction band can then recombine with these holes, emitting photons with

an energy near the band gap energy. This process can also be stimulated by incoming photons with suitable energy. Most semiconductor lasers are laser diodes, which are pumped with an electrical current in a region where an n-doped and a p-doped semiconductor material meet.

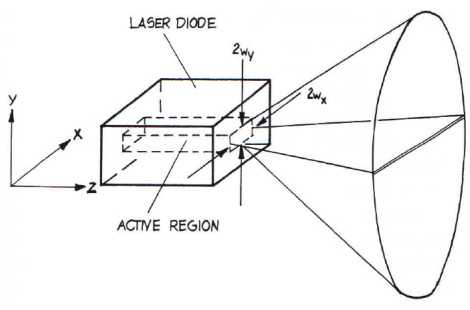

Figure 3.2: Schematic diagram of how a semiconductor laser emits a quasi-elliptical output beam because of the asymmetrical beam confinement in 2 orthogonal directions inside the laser diode.

While the most common semiconductor lasers are operating in the near-infrared spectral region, some others generate red light (e.g. in GaInP-based laser pointers) or blue or violet light (with gallium nitrides). For mid-infrared emission, there are e.g. lead selenide (PbSe) lasers (lead salt lasers) and quantum cascade lasers.

3.1.1 External cavity diode lasers (ECDLs)

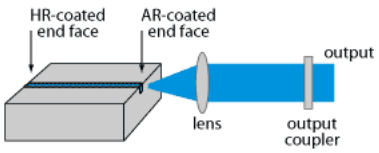

Figure 3.3: Simple setup of a diode laser with external cavity. The semiconductor chip is anti-reflection coated on one side, and the laser resonator extends to the output coupler mirror on the right-hand side.

An external-cavity diode laser is a semiconductor laser based on a laser diode chip which typically has one end anti-reflection coated, and the laser resonator is completed with, e.g., a collimating lens and an external mirror as shown in Fig. 3.3. The external laser resonator introduces various new features and options:

- The longer resonator increases the damping time of the intra-cavity light and thus allows for lower phase noise and a smaller emission linewidth.

- An intra-cavity filter such as the diffraction grating can further reduce the linewidth. Typical linewidths of external-cavity diode lasers are below 1MHz.

- Wavelength tuning is possible by including some adjustable optical filter as tuning element. Most often, a diffraction grating is used for this purpose.

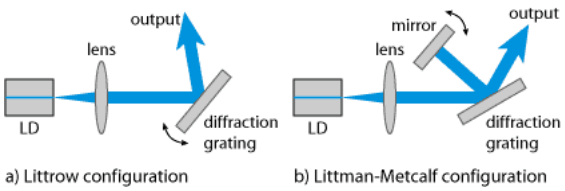

Figure 3.4: Tunable external-cavity diode lasers in Littrow and Littman–Metcalf configuration.

Tunable external-cavity diode lasers usually use a diffraction grating as the wavelength-selective element in the external resonator and because of that they are also called grating-stabilized diode lasers. The common Littrow configuration (see Fig. 3.4) contains a collimating lens and a diffraction grating as the end mirror. The first-order diffracted beam provides optical feedback to the laser diode chip, which has an anti-reflection coating on the right-hand side. The emission wavelength can be tuned by rotating the diffraction grating. A disadvantage is that this also changes the direction of the output beam, which is inconvenient for many applications. In the Littman–Metcalf configuration (see Fig. 3.4), the grating orientation is fixed, and an additional mirror is used to reflect the first-order beam back to the laser diode. The wavelength can be tuned by rotating that mirror. This configuration offers a fixed direction of the output beam, and also tends to exhibit a smaller linewidth, as the wavelength selectivity is stronger. (The wavelength-dependent diffraction occurs twice instead of once per resonator round trip.) A disadvantage is that the zero-order reflection of the beam reflected by the tuning mirror is lost, so that the output power is lower than that for a Littrow laser.

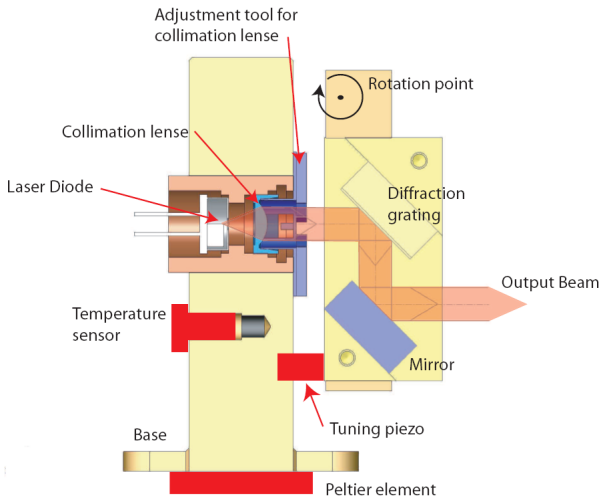

Figure 3.5: Cross-section through the Diode laser head. The Littrow grating is held in separate block opposite to diode output. Frequency control is done by a piezo induced rotation of the grating. The 0th order output beam is deflected to avoid beam walk under frequency tuning. Temperature control ensures stable operating conditions.

3.1.2 Diode lasers used in the student lab

You will use two home built diode lasers during the course of this experiment. One diode laser provides the laser light to address the **cooling transition** $|F = 3, m_F = 3\rangle \rightarrow |F' = 4, m_F = 4\rangle$ of ^{85}Rb, with an AOM added slight detuning from resonance to fulfill the red detuning condition (§ 2.3) required for the correct functioning of the MOT. Since the atoms can be off-resonantly excited by this laser to the other allowed transitions (§ 1.6) from $|F = 3, m_F = 3\rangle$, part of the atoms are lost from the cooling cycle at each absorption, thus leading to a progressive effective atom loss. To prevent this the cooling scheme has to be a closed cycle and this is achieved for alcali atoms by adding just another laser that addresses the lost atoms, bringing them back into the cooling cycle. Thus the second laser is tuned to the **repumping transition** $|F = 2, m_F = 2\rangle \rightarrow |F' = 3, m_F = 3\rangle$ of ^{85}Rb. The laser diode of each laser is mounted into a solid aluminium holder which carries the laser diode and a collimation lens (see Fig. 3.5). To fulfill the **Littrow criterion** [8] the diode is mounted opposite a holographic grating and a deflection mirror. Both of them are glued into a separate aluminium block, which is attached to the main holder via springs and three precision screws (see Fig. 3.6). For shielding against convection and atmospheric pres-

sure fluctuations the laser is mounted in a sealed aluminium box which is bolted to the optics table.

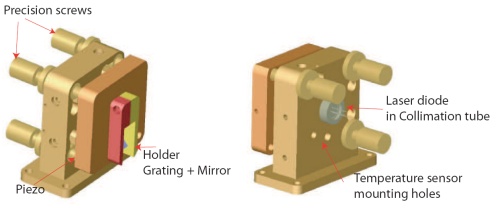

Figure 3.6: Schematic of front and rear view of our homebuilt ECDL setup.

The laser light is generated by sending a current through the active region of the diode between the n- and p-type cladding layers. This produces electrons and holes, which gradually recombine and thus emit photons. The laser's emission wavelength is determined by the band gap of the semiconductor material and is very broadband (in our case 7 nm) relative to atomic transitions. The chosen low cost laser diode is also used in CD-R drivers. It is plugged inside a collimation tube which houses a collimation lens. The aperture and the focal length of the lens are adapted to the opening angles of the diode output beam. This is necessary because the light leaving the diode is emitted from a small rectangular region (typically on the order of $0.1\mu m$ by $0.3\mu m$) leading to a diverging output of a laser diode. A typical output beam has a divergence angle of 30° in the direction perpendicular to the junction, and 10° in the parallel direction [9]. If the laser is operating in a single transverse mode, the collimated beam is elliptical, but it can be made nearly radially symmetric by using anamorphic prisms (§ 3.3.2).

The grating is a holographic gold coated sine grating with a grating constant of 1800/mm to meet the Littrow condition. In this arrangement, the light diffracted from a grating is coupled back into the diode, so that the grating and the diode's rear facet form an external resonator. The diode chip, with its reflecting facets, acts like an intracavity etalon and the external diffraction grating selects a single-mode of the chip. The use of a grating results in a linewidth reduction of two orders of magnitude [8]. For good grating illumination, the diode orientation is adjusted such that its elliptic beam profile is perpendicular to the groove orientation (i.e. polarisation parallel).

For a coarse adjustment of the laser frequency, the laser can be scanned by the corresponding precision screw which provides a vertical tilt of the grating holding block (this was done by the tutors, when setting up the experiment; during the lab course the laser head will not be accessible). In the operational mode the tilt of the grating holding block is realized by means of voltage ramp

applied to a crystal mounted underneath the tip of this precision screw. The stacked piezo crystal has a maximum stroke of $5\mu m$ and in this configuration results in a tuning of roughly 125MHz per Volt. To control the offset voltage of the piezo a Thorlabs piezo controller is used (Thorlabs MDT693A , see Fig. 3.7).

Figure 3.7: Picture of the Piezo Controller MDT693A used to control offset voltage of the piezo.

A fraction of the beam incident on the grating is reflected out of the external resonator (0th order) by hitting a mirror parallel to the grating (see Fig. 3.4). This constitutes the output of the stabilized laser. The grating constant is chosen such that the angle between incident beam and 0th order is close to 90 degrees. Under frequency tuning, the mirror co-rotates with the grating and ensures stable beam pointing.

The whole setup is temperature stabilized by a Thorlabs temperature controller (Thorlabs TED200, see Fig. 3.8) and a Peltier element. During the experiment you won't need to change the set values of this values because the optimal temperature set point was already fixed by the tutors.

Figure 3.8: Picture of the Thermoelectric Temperature Controller TED200 used to stabilize the temperature of the laser diode.

The laser diode current is supplied by a commercial diode current controller (Thorlabs LDC2000, see Fig. 3.9). Before entering the diode, the current passes a small electronics board, mounted inside the laser box which serves many purposes. The circuit board possesses components to protect the laser diode: three safety diodes, connected in parallel with the laser diode, prevent the laser diode from being exposed to over-voltages, then a choke smooths the laser current to avoid destructive voltage spikes and finally a Schottky diode is used against accidental reversed voltages.

Figure 3.9: Picture of the Laser Diode Controller LDC202C used to stabilize and control the current fed the laser diode.

3.2 Laser locking

The lasers in the student lab have to run at a constant frequency which is often equal to an atomic transition. Unavoidable thermal fluctuations, acoustic and electronic noise change the frequency of the laser and these changes are undesired, so they have to be corrected by stabilizing the laser to a specific frequency ("Laser locking"). To achieve this the frequency of emission of the laser has to be dynamically adjusted to compensate its drifts and fluctuations by controlling the angle of the external cavity grating via the piezo electric crystal and/or by changing the laser's input current. The amount of correction to be applied to these two control parameters is calculated and generated by an appropriate feed-back circuit (e.g. a PID controller) which requires as input a control variable. This control variable is compared to the set point stored in the feed-back circuit and from this difference is originated the error signal that first will be processed and then applied to the control parameters.

To achieve a correct feedback the error signal should be proportional to the difference between the set point (the desired frequency) and the current position (the actual laser frequency). Additionally it has to change sign if the deviation is going in one or the opposite direction. When the difference becomes zero, the error signal is equal to zero and the laser frequency is the same as the atomic transition frequency.

A good choice for the control variable is to use the signal obtained from the FM spectroscopy (§ 1.7), which represents effectively the derivative of the absorption spectrum. The shape of the FM-spectroscopy signal can be adjusted by varying the phase shift to reproduce as well as possible the derivative of the atomic spectrum. This means that when the value of the FM-spectroscopy signal is zero then the laser frequency is at the middle of the resonance. If the laser frequency is shifted from the atomic resonance, the FM-signal has a positive value at one side of the resonance and a negative value at the other one. The value of the FM-signal is also nearly proportional to the frequency difference for small shifts.

In the lab, this is done by sending the FM-signal first to a PI (propor-

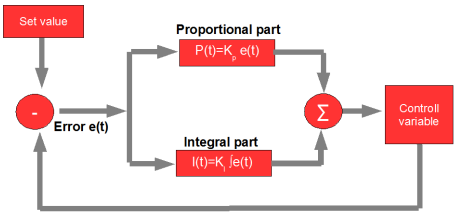

Figure 3.10: Principle of a PI-Controller.

tional–integral) controller. The PI loop is extensively studied at the FP-E01 Elekronik Grundpraktikum, so we will refer to the instruction and the references therein and give here only a very basic introduction. A PI-controller compares the actual value of a control variable with the set value. If the control variable is not equal to the set value, the (time dependent) error-function is non zero. The error-function is split in two different parts: a proportional part, where the output is proportional to the value of the error function, and a integral part, which integrates the error-function over a certain time. The outputs of the two paths are combined afterwards and the resulting signal is sent as a feedback to the control variable (see Fig. 3.10). In our case the control variable is the signal obtained from FM spectroscopy (§ 1.7). Since we want stabilize the frequency to an atomic resonance (where the FM-signal is zero) we have to set the set value of the PI loop to zero. If the Laser is not on resonance, the error function is thus non-zero and a P-part and (normally also the I- part) is non-zero and the output of the PI loop differs from zero. The PI-output is sent to the piezo controller, which corrects the laser wavelength by changing the angle of the grating (see Fig. 3.11).

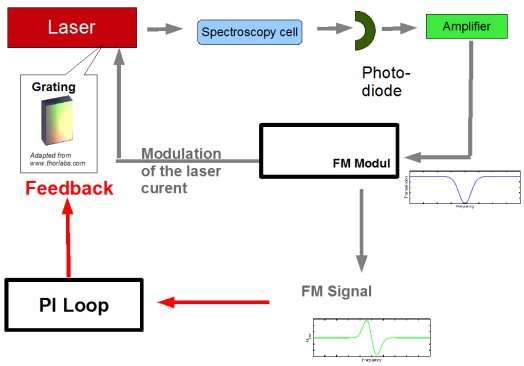

Figure 3.11: Principle of locking the laser via FM spectroscopy.

The lasers in the student lab run with an accuracy of the order of one MHz, which is less than the natural linewidth of the atomic transition. Since the frequency of the laser itself is in the order of 10^{14} Hz, the relative accuracy is of the 10^8 order.

3.3 Optical Setup

3.3.1 Introduction

The laser system of the setup is based on two independent diode lasers which generate the light for the MOT. One produces the light for cooling ("Cooler") the atoms and the other one is used for bringing the atoms back into the cooling cycle, if they fall into the "wrong" hyperfine state ("Repumper").

An overview of the optical paths is given in the photos and the different optical components are explained in the following sections.

The optical paths are already aligned and you shouldn't change them without your advisor!

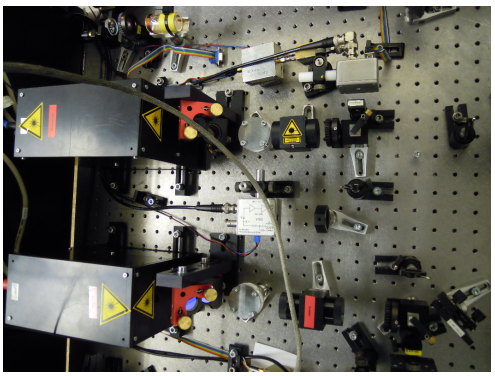

Figure 3.12: Laser system for the FP experiment.

3.3.2 Anamorphic Prism Pair

A laser beam emitted from a diode laser (§ 3.1.2) has an elliptical beam profile. A round beam profile can be created when one principle axis is magnified by the ratio of the beam diameters of the two principal axises. If a beam of parallel monochromatic light passes through a prism (unless the prism is used in the symmetrical minimum-deviation position) the width of the beam will be increased or decreased in one dimension, as illustrated

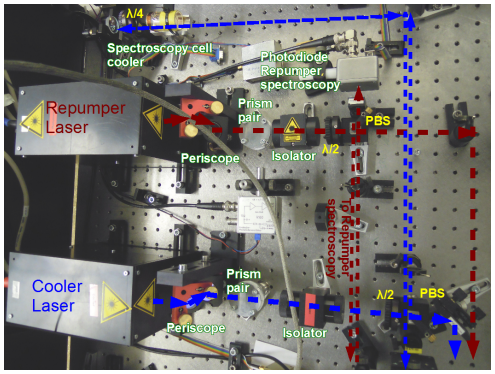

Figure 3.13: Beam paths after the lasers.

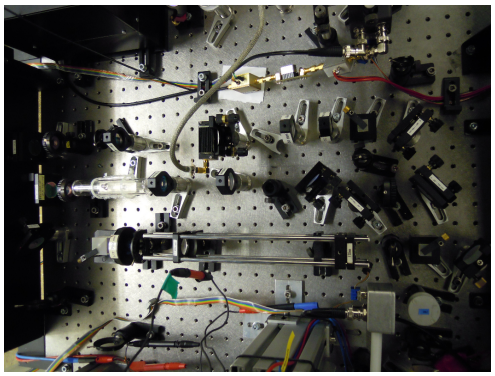

Figure 3.14: Optical system for preparing the right frequencies and beam diameters.

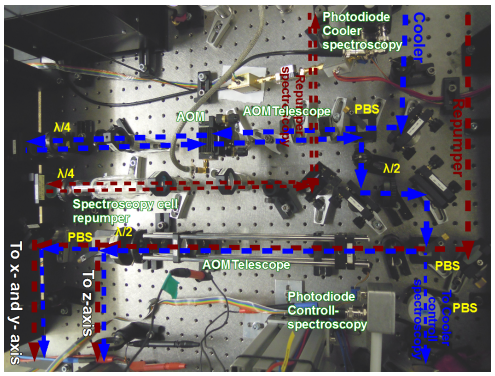

Figure 3.15: Beam paths in the middle section.

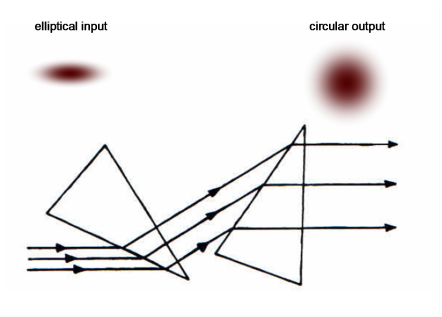

Figure 3.16: One-dimensional beam expansion without beam deflection using two oppositely oriented anamorphic prisms.

in Fig. 3.16. By using two identical prisms in an inverted configuration, compression or expansion can be accomplished without inducing an angular change in the beam direction. Such prism pairs can be used, in conjunction with lenses, to produce anamorphic laser beam expanders.

3.3.3 Optical Isolator

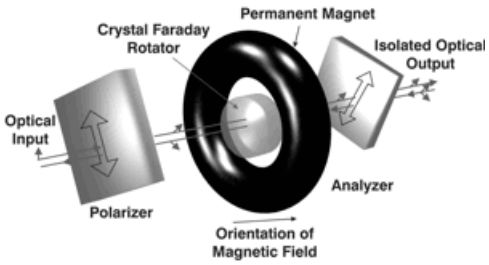

Figure 3.17: Optical isolator that uses two linear polarizers and a Faraday material producing a 45° polarization rotation.

Back reflections from different optical components onto the laser diode (§ 3.1.2) lead to instabilities in the laser performance or can even destroy the diode. Such back reflections can be easily avoided by installing an optical isolator (or Faraday isolator) directly after the laser head.

The simplest type of Faraday isolator is polarization-sensitive in the sense that it works only when the input beam has a prescribed direction of linear polarization. Here, a properly polarized and collimated input beam passes a first polarizer (pol 1 in Fig. 3.17) with minimum loss, then a 45° Faraday rotator, and finally another polarizer (pol 2) with its transmitting axis being

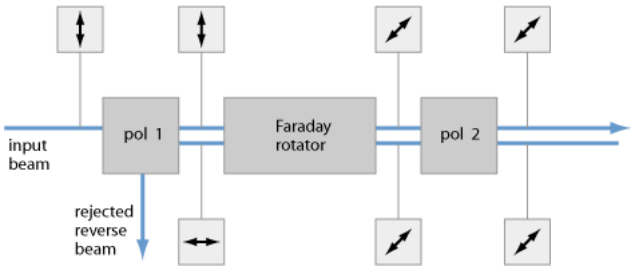

Figure 3.18: Setup of a polarization-sensitive Faraday isolator. The double arrows indicate the polarization directions of a forward and backward-propagating beam.

rotated by 45°, such that the transmission losses are small. When light is reflected back to the output port of the isolator with an unchanged polarization state, it can fully transmit through the output polarizer (pol 2). Then, however, its polarization direction is rotated by another 45° in the Faraday rotator, so that this light will be blocked at the input polarizer or be sent to a separate output port. Note that the output polarizer (pol 2) is important if light is reflected back with a modified polarization state.

3.3.4 Wave plates

Wave plates (retardation plates or phase shifters) are made from materials which exhibit birefringence. The velocities of the extraordinary and ordinary rays through the birefringent materials vary inversely with their refractive indexes. The difference in velocities gives rise to a phase difference when the two beams recombine. In the case of an incident linearly polarized beam this is given by $\Delta\phi = \frac{2d(n_e - n_o)}{\lambda}$ (with $\Delta\Phi$ = phase difference; d = thickness of wave plate; n_e, n_o = refractive indexes of respectively extraordinary and ordinary raysλ = wavelength). At any specific wavelength the phase difference is governed by the thickness of the retarder. Note that when a light beam is linearly polarized and the polarization direction is along one of the axises of the wave plate then the polarization remains unchanged.

$\lambda/2$ wave plate

The thickness of a half-wave plate is such that the difference in the optical pathways is 1/2 wavelength or 1/2+n wavelengths (where n is an integer number). This corresponds to a phase difference of π.

A linearly polarized beam incident on a half wave plate emerges as a linearly polarized beam, but rotated such that its angle to the optical axis

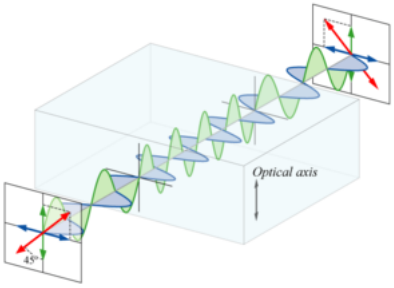

Figure 3.19: A half-wave plate. Linearly polarized light entering a wave plate can be resolved into two waves, parallel (shown as green) and perpendicular (blue) to the optical axis of the wave plate. In the plate, the parallel wave propagates slightly slower than the perpendicular one. At the far side of the plate, the parallel wave is exactly half of a wavelength delayed relative to the perpendicular wave and the resulting combination (red) is orthogonally polarized compared to its entrance state.

is twice that of the incident beam. Therefore, half wave plates can be used as continuously adjustable Polarization rotators. Half wave plates are used to rotate the plane of Polarization and as a variable ratio beamsplitter when used in conjunction with a Polarization cube.

$\lambda/4$ wave plates

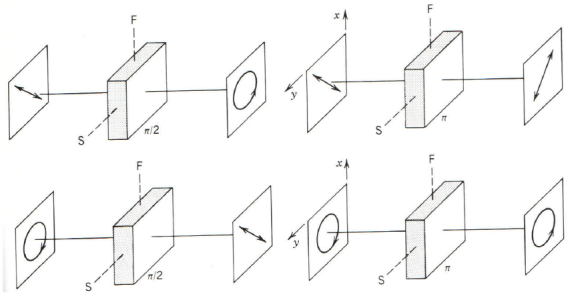

Figure 3.20: Inner working of a quarter wave and a half wave plate. F and S represent the fast and the slow axis of the retarder respectively.

The thickness of the quarter wave plate is such that the difference in the optical pathways is 1/4 wavelength or 1/4+n wavelengths. The corresponding phase difference is $\pi/2$.

If the angle q (between the electric field vector of the incident linearly polarized beam and the retarder principal plane) of the quarter wave plate is

45°, the emergent beam is circularly polarized. When a quarter wave plate is double passed, i.e. by mirror reflection, it acts as a half wave plate and rotates the plane of Polarization to a certain angle. In the setup, quarter wave plates are used for creating circular Polarization of the MOT beams that enter the vacuum chamber. Moreover they find application in the AOM double pass (§ 3.3.9) as well as in the spectroscopy path (§ 3.3.7). In these applications they are passed twice, so that they effectively act as a half wave plate.

3.3.5 Beamsplitter

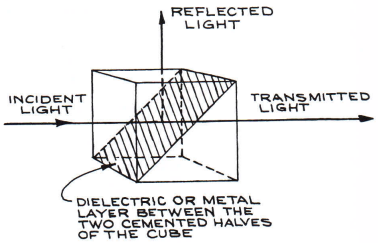

Figure 3.21: Polarizing beamsplitter cube.

The ratio of reflectance to transmittance of a beamsplitter depends on the polarization state of the light. The performance is usually specified for light linearly polarized in the plane of incidence (P-polarization) or orthogonal to the plane of incidence (S-polarization). Cube beamsplitters are pairs of identical right-angle prisms cemented together on their hypotenuse faces. Before cementing, a metal or dielectric semi reflecting layer is placed on one of the hypotenuse faces. The operation of a beamsplitter is illustrated in Fig. 3.21. By placing a wave plate in front of the so called polarizing beamsplitter cube (PBS) the branching ratio between the transmitted and reflected beam can be easily adjusted. For instance the three retro reflected MOT beams should be split in the ratio 2:1:1 (z:y:x) in this way.

3.3.6 Laser beam expansion

Laser beams can be expanded and recollimated (or focused and recollimated) with simple or Galilean telescope arrangements, as illustrated in Fig. 3.22. A Galilean telescope has the advantage that the laser beam is not brought to an intermediate focus inside the beam expander. Since lasers

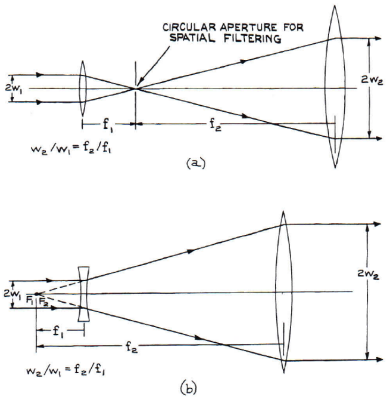

Figure 3.22: Laser beam expanders: (a) focusing type with optional optical filter implementation. (b) Galilean Telescope.

beams are highly monochromatic, beams expanders don't have to be constructed from achromatic lenses. In order to save space mostly Galilean telescopes are used in the laser system.

Telescopes can also be realized with two positive lenses (Kepler Telescope), producing a true laser focus at the intersection of the two foci. If a small circular aperture is placed at the common intermediate focus of such a simple-telescope beam expander, the device becomes a spatial filter as well.

In order to get a stronger spectroscopy signal a Galilean telescope is used in the spectroscopy path (§ 3.3.7). This way the beam size inside the Rb vapor Cell can be enlarged. Before entering the Vacuum chamber (§ 3.4) the overlapped cooling and repumping beams are also enlarged by a Kepler Telescope to increase the cooling and trapping region of the MOT.

The $1/e^2$ diameter of the MOT beams is 20 mm and the power per beam is circa 2.5-3 mW (you have to measure this power during the experiment).

3.3.7 Spectroscopy path

The optical system also features a so called spectroscopy path that allows to do Doppler free saturated absorption spectroscopy (§ 1.4). This is necessary to lock (§ 3.2) the two diode lasers (§ 3.1.2) to atomic transitions to successfully operate the MOT. Using a half wave plate (H) (§ 3.3.4) and a polarizing beam splitter (PBS) (§ 3.3.5) a small fraction of the beam is reflected into the spectroscopy path. A Galilean Telescope (GT) (§ 3.3.6) expands the beam before it enters a Rb vapor cell containing both isotopes of rubidium (^{85}Rb and ^{87}Rb). The beam expansion is done to increase the

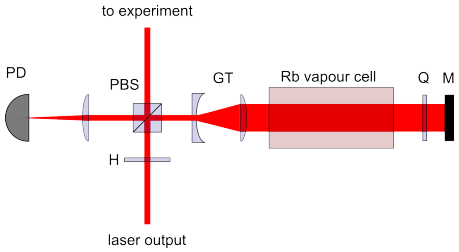

Figure 3.23: Schematic sketch of the spectroscopy path. PBS = polarizing beam splitter, GT = Galilean Telescope, H = half wave plate, Q = quarter wave plate, M = mirror.

number of atoms that contribute to the spectroscopy signal and to keep at the same time the total laser power very low to prevent power broadening (§ 1.4). After a first passage through the vapor cell, the laser beam passes a quarter wave plate (Q) (§ 3.3.4) and is afterwards retro-reflected by a mirror (M). The quarter wave plate induces a 90° rotation of the laser beam polarization such that the retro-reflected light can exit the polarizing beam splitter to finally illuminate a photodiode (PD). In this case the retro-reflected laser beam acts as a "probe beam" which probes the zero velocity class atoms that have been excited by the "pump beam". This reveals the so called lamb dips (§ 1.4). The photodiode signal is finally fed into the locking electronics of the cooling or repumping lasers to allow laser frequency stabilization through the Frequency Modulation scheme (§ 1.7).

3.3.8 Photodiode

The photodiode in the setup is used for measuring the atom number via the fluorescence. This is done in the following way: Depending on the laser detuning in respect to the resonance and on the laser intensity, an atom scatters a certain amount of photons per time unit. The scattering process is isotropic and (depending on the collected solid angle of the emission) a certain amount of photons reaches the photodetector, where the photon power is converted into an electrical voltage. The conversion table (which depends on the resistor, in our case 10 MOHM) can be found in the photodiode manual (Thorlabs PDA36A).

3.3.9 Acousto-optic modulator (AOM)

An acousto-optic modulator (AOM) is a device which can be used for controlling the power, frequency or spatial direction of a laser beam with

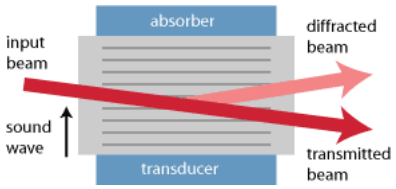

Figure 3.24: Schematic setup of an acousto-optic modulator. A transducer generates a sound wave, at which a light beam is partially diffracted. The diffraction angle is exaggerated.

an electrically driven signal. It is based on the acousto-optic effect, i.e. the modification of the refractive index by the oscillating mechanical pressure of a sound wave.

The key element of an AOM is a transparent crystal through which the light propagates. A piezoelectric transducer attached to the crystal is used to excite a sound wave with a frequency between 60 and 150 MHz. Light can then experience Bragg diffraction at the periodic refractive index grating generated by the sound wave. The scattered beam has a slightly modified optical frequency (increased or decreased by the frequency of the sound wave) and a slightly different direction.

The frequency and direction of the scattered beam can be controlled via the frequency of the sound wave, whereas changing the acoustic power allows to control the optical power. For sufficiently high acoustic power, more than 70% of the optical power can be diffracted.

The acoustic wave may be absorbed at the other end of the crystal. Such travelling-wave geometry makes it possible to achieve a broad modulation bandwidth of many Megahertz. Common materials for acousto-optic devices are tellurium dioxide (TeO2), crystalline quartz, and fused silica.

In practice we use an AOM to change the frequency of the cooling laser. This becomes especially important on the third day of the lab course (§ 4.2.3), when you have to record the number of trapped particles with respect to the detuning of the cooling laser.

Important parameters

Deflection: a diffracted beam emerges at an angle θ that depends on the wavelength of the light λ relative to the wavelength of the sound λ_s

$$\sin\theta = \left(\frac{m\lambda}{2\Lambda}\right) \tag{3.1}$$

in the Bragg regime and

$$\sin\theta = \left(\frac{m\lambda_0}{n\Lambda}\right) \tag{3.2}$$

with the light : normal to the sound waves, where $m = ..., -2, -1, 0, 1, 2, ...$ is the order of diffraction.

Intensity: the amount of light diffracted by the AOM depends on the intensity of the sound wave. Hence, the intensity of the sound can be used to modulate the intensity of the light in the diffracted beam. Typically, the intensity that is diffracted into $m = 0$ order can be varied between 15% to 99% of the input light intensity. Likewise, the intensity of the $m = 1$ order can be varied between 0% and 80%80. In the FP setup, the modulation strength is optimized such that 80% of the light is diffracted into the +1st order

Frequency: one difference from Bragg diffraction is that the light is scattered from moving planes. A consequence of this is that the frequency of the diffracted beam f in order m will be Doppler-shifted by an amount equal to the frequency of the sound wave F.

$$f \rightarrow f + mF \tag{3.3}$$

This frequency shift is also required by the fact that energy and momentum (of the photons and phonons) are conserved in the process. A typical frequency shift varies from 50 MHz, for a less-expensive AOM, to 400 MHz, for a state-of-the-art commercial device. In some AOMs, two acoustic waves travel in opposite directions in the material, creating a standing wave. Diffraction from the standing wave does not shift the frequency of the diffracted light.

Double pass configuration

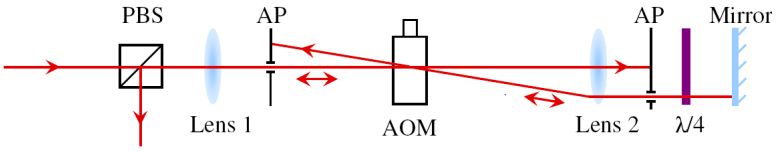

Figure 3.25: AOM alignment for double passed light, PBS = polarizing beam splitter; AP = aperture; AOM = acousto-optic modulator; $\lambda/4$ = quarter wave plate.

When a laser's frequency is scanned with an AOM, the angle of the first-order diffracted beam shifts as well, since the beam direction angle is a function of modulation frequency. For many applications this beam shift is an unwanted side effect and, when changing the frequency of the AOM, would severely influence the optical alignment of the beam through the following optics. This change in the diffraction angle can be effectively compensated by using the AOM in the double-pass configuration. Here the output of the m^{th} order of the AOM is retro-reflected for a second pass through the AOM leading to a frequency offset of $2m\Delta f$ on the double passed beam. In this arrangement changing the frequency of the acoustic wave (by Δf), and hence the frequency of the detected light, does not cause any steering of the first order output of the second pass. The output of the second pass counter-propagates with the original input beam. While this is desirable, as it allows the frequency to be changed without any steering of the output beam, it poses the problem of how to separate the path of the output beam from that of the input beam. A $\lambda/4$ wave plate (§ 3.3.4) is placed just before the mirror and causes the second pass of the AOM to be orthogonally-linearly polarized with respect to the first pass. This allows the beam paths to be separated using a polarizing beam splitter (§ 3.3.5).

3.4 Vacuum system

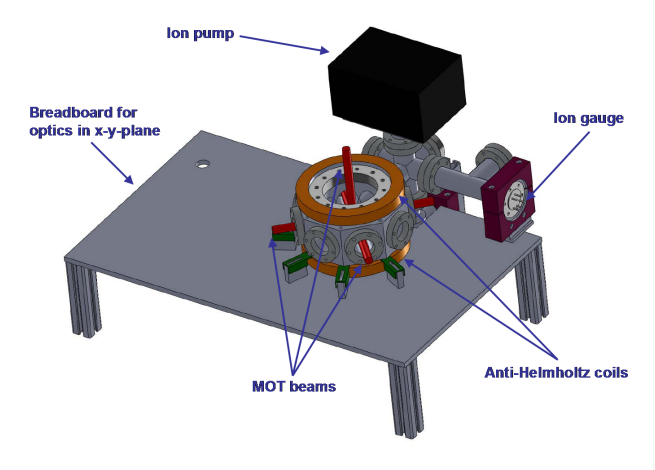

Figure 3.26: Top view of the ultrahigh vacuum system.

Perfect thermal isolation between a gas sample and the material of walls surrounding it has enabled experiments with ultracold atomic and molecular

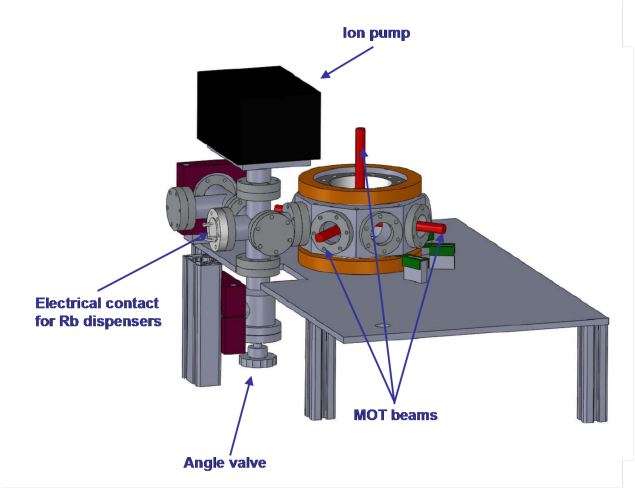

Figure 3.27: Side view of the ultra-high vacuum system.

gases to take place in an apparatus kept at room-temperature. It is remarkable that it is for example even possible to maintain a Bose-Einstein condensate (BEC) for many seconds in a machine that is warmer by a factor of 10^9 than the gas sample. No heating due to the hot walls is detectable unless the atoms approach a metal surface within microns. Transfer of energy from the walls to the gas sample may take place through two channels: through the room-temperature black body radiation field and through gas molecules. Atomic gases couple extremely weakly to the room-temperature black body radiation field, which leaves most experiments in the rest-gas limited regime. The best condition for any experiment with trapped cold gases is therefore an ultra-high vacuum (UHV) environment (UHV is defined as the region of pressure below 10^{-8} mbar). By relatively simple means, one can now produce a laboratory vacuum which has a pressure of 10^{-11} mbar, comparable to the interplanetary medium. In this regime the "residual gas" normally consists of atoms and molecules which mostly reside on the walls, but that occasionally come off and fly ballistically through the vacuum system with an energy corresponding to the wall temperature. These residual gas particles therefore have an energy that is many orders of magnitude above that of the ultracold gas sample, and even "grazing" collisions will knock particles out of the sample, giving rise to direct loss rather than heating.

The ultra high vacuum (UHV) system you will work with during the next week was machined in the mechanical workshop of the Physics Institute. It has an octagon shape featuring ten viewports, of which nine are optically accessible. The tenth viewport, which is not optically accessible, connects to the Ion pump that is necessary to maintain a background pressure of

$1.6 \cdot 10^{-9}$ mbar. This pressure can be measured through an ion gauge, that is also connected to the UHV system. The vacuum chamber houses inside two Rb-dispensers. When a current (6A - 8A) is sent through them, they emit hot Rb atoms of both stable Rb isotopes. This 700 K background gas will then be cooled by the three mutually orthogonal and counter-propagating cooling beams that form the MOT. Additionally, the vacuum chamber supports a pair of **Anti-Helmholtz coils**, that provide the required magnetic field gradients which are necessary for successful atom trapping. The entire chamber is mounted on a 50 x 75 cm breadboard on which the optics for the cooling and repumping laser beams are mounted. **During the course of your lab work you are only allowed to adjust the optical components in the direct vicinity of the chamber, since the remaining optics are already aligned by the tutors.**

Each Anti-Helmholtz coil consist of 90 windings, and the coils produce gradients of 1.25 G/A/cm. The coils have a diameter of about 170 mm and have a distance of about 115 mm. They aren't actively cooled, so you shouldn't run currents higher than 6A through them to avoid overheating and possibly a meltdown of the glue that is holding them.

Chapter 4

Work instructions

The experiment is located in room 01.415 on the first floor of the Physics Institute at Im Neuenheimer Feld 226. Before you start the lab course you have to meet your tutors in front of the laboratory, you need to learn the safety instructions and then you have to follow the work instructions. The experiment can be carried out in two full days of 8 hours each or in four afternoons of 4 hours each, other arrangements are possible only by previous agreement with the tutors.

4.1 Safety Issues

This student lab provides an exciting experiment in which you can work with tools that can be found in all the experiments which deal with ultracold atoms. The aim of this experiment is to allow you to learn this techniques from scratch and to play around with atoms, which will be at a temperature of only a few hundred micro kelvin higher than the absolute zero temperature point.

But when working with the MOT setup you have to deal with technical devices which can cause dangers to your health, if you don't work carefully and if you don't respect the basic safety rules of a modern optics lab!!! You had to sign that you got the introduction in laboratory and laser security during the "Sicherheitsbelehrung" and you have to take this seriously!

Besides some general rules working, the FP20 course has some specific safety issues, in particular lasers and high electrical voltages and currents, which we describe here in detail.

4.1.1 General rules

- **Never work alone** in the lab. Make sure that there is **always a second person** with you, with which you can discuss dangers and working strategies.
- **Never work in the lab under the influence of alcohol, drugs or strong medicaments.**
- Always contact the lab assistant if you have the slightest doubts about any safety issues or the destruction of any lab equipment.

4.1.2 Laser safety

To realize a MOT a certain laser power is necessary. The lasers used in the student lab are all classified in the highest laser-protection class ("Laserschutzklasse 4"). This section is intended to introduce you to the very basic rules of working safely with the lasers used in this experiment. Obeying to the rules stated here is absolutely necessary to exclude the risk of severe injury.

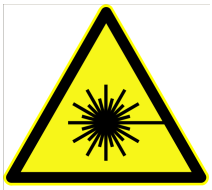

Figure 4.1: Official laser warning sign.

In this experiment you will be using diode lasers that emit a light power of up to 50 mW. This power is at least ten times higher than the one emitted from a common laser pointer. The fact that the wavelength of the light used here ($\lambda = 780$nm) is in the near infrared (NIR), requires even grater caution because the beam path is (almost) invisible to the naked eye. The beams can only be made visible by means of additional equipment such as IR-viewers, viewer cards or CCD-cameras. The laser powers are not high enough to cause injury to exposed skin; they are, however, strong enough to heat up the retina of the human eye very quickly if exposed to the beam. This is particularly dangerous in the case of IR light, because the receptors are insensitive at those wavelengths and none of the automatic protection mechanisms such as eye lid or iris closing works. A heated retina part will very rapidly be irreversibly destroyed which will lead to blind spots in the

vision or even to full blindness of the eye. The above implies the following rules:

- **Wear protection glasses** (available in the lab) all the time.
- **You'll be not allowed to continue the measurements, if one of the advisors will see you without glasses!**
- **Do not wear jewelery, watches** or any other possible reflecting objects on your arms, wrists, hands, and fingers while aligning optics. It is a good practice to take them off during the whole time spent in the laboratory, this way you'll avoid the risk of forgetting to take them off when you'll need to work with the lasers.

Figure 4.2: Laser safety goggles for 780nm light.

In addition to these rules concerning your personal safety, we would like to state an additional set of rules meant to protect the more delicate of the technical equipment used in the experiment. Especially laser diodes are very sensitive instruments that can be damaged easily. If this happens the FP-Mot will not be operational for a long period! Therefore please:

- Always contact a lab assistant when you are not sure about any manipulation of the laser setup.
- Do not change the temperature of the lasers on your own. And please never switch the temperature controllers off!
- Only change the laser current by small amounts when the spectroscopy runs badly. Do so only if you have received a detailed introduction on how to operate the current drivers.
- Do not try to do any mechanical adjustment on the lasers and their housings.

When you start to work with the lasers, please follow the following procedure:

- **First** switch on the the **piezo controller** (Thorlabs Piezo Controller MDT693A) (§ 3.1.2).

Figure 4.3: Picture of the Laser Diode Controller LDC202C used to stabilize and control the current fed to the laser diode.

Figure 4.4: Picture of the Piezo Controller MDT693A used to control offset voltage of the piezo.

- **Then** switch on the the **current controller** of the laser diode (Thorlabs Laser Diode Controller LDC202C) (§ 3.1.2).

If you switch off the diode lasers before leaving the lab, please **first** switch off the **current controller** of the laser and then switch off the **piezo controller**.

4.1.3 Electronic danger

- Please keep in mind that the piezos (§ 3.1.2) by which the laser wavelength is scanned need **high voltages**! So **never disconnect the BNC cables** from the piezo controller, while the piezo controller is on, neither touch them.

- When working with the rubidium dispensers, please make sure that the **banana cables are connected to the power supply**. The dispensers will need up to 7A to provide the required atom flux. Before switching on the power supply, make sure that the adjustment knobs are turned down to 0. After having switched on the power supply, please gently increase the current flowing through the dispensers. When you finish the lab day, please make sure that the dispensers are switched off. Note that the dispensers only have a limited amount of Rubidium. Once the sources are extinguished, they have to be replaced. This means that the vacuum chamber needs to be opened and later on backed out again. This procedure will take up to six weeks!

- For successful atom trapping you also need a magnetic field generated

by **magnetic coils**. Please make sure that the **banana cables are connected to the power supply**. The coils will be operated between 3.5A and 6A to provide the required magnetic field gradients. Before you switch on the power supply, make sure that the adjustment knobs are turned down. After having switched on the power supply, please gently increase the current flowing through the coils. When searching for the MOT you will need to find the correct current direction. This means that you most likely have to reverse the polarity of the coils. When doing so, always switch off the power supply before changing the banana plugs. Note that the high current flowing through the coils heats them up significantly. So please check the produced heat every now and then, to ensure that the plastic around the coils does not melt.

4.2 Work Instructions

4.2.1 Day 1

Colloq Part I

The FP20 colloquium is split into two short parts, which take place at the beginning of Day 1 and Day 2. By this we can separate the two main theory sections of this lab course, namely **Doppler free spectroscopy** and **laser cooling**. To prepare for the colloquium you need to know details about:

1. Basic laser absorption spectroscopy
2. Saturated absorption and Doppler free spectroscopy
3. Energy levels of Rubidium
4. Frequency modulation (FM) spectroscopy

Lab instructions

After having passed the colloquium you will have time to get used to the basic monitoring and controlling units in the optics lab, especially the ones of the lasers and of the spectroscopy. If you feel comfortable with the electronics you have to **Record the D2-line spectra of both Rubidium isotopes**. To do so you can use the USB port of the digital oscilloscope in the lab. You should record the spectrum of both cooler and repumper lasers and then analyse only the best set between the two. You have to take the following data:

Together (on the same scan, with the end of the two absorption profiles well inside the scan range) the:]

- $^{87}Rb\ F = 2 \rightarrow F'$ and $^{85}Rb\ F = 3 \rightarrow F'$ transitions
- $^{85}Rb\ F = 3 \rightarrow F'$ and $^{85}Rb\ F = 2 \rightarrow F'$ transitions
- $^{85}Rb\ F = 2 \rightarrow F'$ and $^{87}Rb\ F = 1 \rightarrow F'$ transitions

From these datasets, by comparing the distance between the centers of the two profiles, you can measure the multiplet separation.

A separate scan of (with the end of the absorption profile well inside the scan range):

- $^{87}Rb\ F = 2 \rightarrow F'$ transitions
- $^{85}Rb\ F = 3 \rightarrow F'$ transitions
- $^{85}Rb\ F = 2 \rightarrow F'$ transitions
- $^{87}Rb\ F = 1 \rightarrow F'$ transitions

From these datasets you can measure the natural **line width** of the **hyperfine lines** from the **Lamb dips** and the temperature of the atomic sample from the **Doppler profile**.

A separate zoomed in scan of (with the six transitions inside the scan range):

- $^{87}Rb\ F = 2 \rightarrow F'$ transitions
- $^{85}Rb\ F = 3 \rightarrow F'$ transitions
- $^{85}Rb\ F = 2 \rightarrow F'$ transitions
- $^{87}Rb\ F = 1 \rightarrow F'$ transitions

From these **recorded Doppler free spectra** you can measure the D2 line hyperfine energy level separation (§ 1.6.2).

For all these datasets, to perform the frequency measurements you have to calibrate the horizontal axis, by converting it from time to frequency. If you maintain the scanwidth setting on the PID controller for few datasets, then you can do the calibration once on one of these datasets and use it also for the others, allowing you to measure the frequency of all lines not used for the calibration and to compare them with the theoretical expectation.

The data analysis is properly described in the Spectroscopy data analysis (§ 4.3.2).

4.2.2 Day 2

Colloq Part II

At the beginning of this day, the theory of the MOT will be discussed in detail during a second colloquium. To prepare for the colloquium you need to know details about:

1. Radiative optical forces
2. Optical molasses
3. Magneto-Optical Trap
4. Temperature regimes accessible in laser cooling
5. Trap loading
6. Temperature measurement via release and recapture

The frame of this colloquium will also be used to discuss the characterization measurements of the MOT.

Lab instructions

Beam path characterization

The work in the lab will start with getting accustomed to the optics setup required for the MOT. To do so you should understand the role of all the elements and to be able to follow and to optimize the optical path of the MOT beams. You should measure the laser beams power with a power meter at different important positions.

For the cooling beam:

1. the power going to the spectroscopy
2. the power going to the MOT beam path
3. the power before the AOM
4. the power after the diaphragm which selects the first order of the AOM diffraction (if possible optimize it by slightly adjusting the AOM angle)
5. the power before the fiber
6. the power after the fiber (with repumping beam blocked)

For the repumping beam:

1. the power going to the spectroscopy
2. the power going to the MOT beam path
3. the power before the fiber
4. the power after the fiber (with cooling beam blocked)

For each beam separately you should try to optimize the fiber coupling via a procedure called **"beam walking"** if the power is not above 10.5 mW for the cooler or 2 mW for the repumper.

Alignment of the MOT beams

Now that you have the cooling and repumping beam perfectly overlapped after the fiber, you can proceed by checking and, if required, by adjusting the alignment of the three MOT beams through the vacuum apparatus. First close the two iris diaphragms which are positioned after the fiber output. This will create a small beam which is much easier to align through the vacuum chamber. Two **masks**, on which the center of the viewport is marked, will be available for this purpose and have to be placed on the viewports of the direction you are aligning. You should use the first mirror to align the beam to the first viewport and the second mirror for align the beam to the center of the second viewport. This will be an iterative procedure commonly called **"beam walking"**. At the end you have to realign the retro-reflection with the help of an iris diaphragm. When you are done open the two irises.

Laser locking

When the three MOT beams are well aligned it is time to lock the cooling and repumping lasers to the cooling and repumping transitions, respectively. The transitions are the following: the Cooler laser is locked on the crossover between $F = 3 \rightarrow F = 2$ and $F = 3 \rightarrow F = 4$ levels, while the Repumper on the $F = 2 \rightarrow F = 3$ line. The tutor will help you once in the beginning with the laser locking procedure. To lock the lasers, please follow the following steps:

1. Go to the **"scan mode"** by flipping the **"scan" switch** at the **PID controller**.
2. Increase the gain at the PI controller to its maximum value.

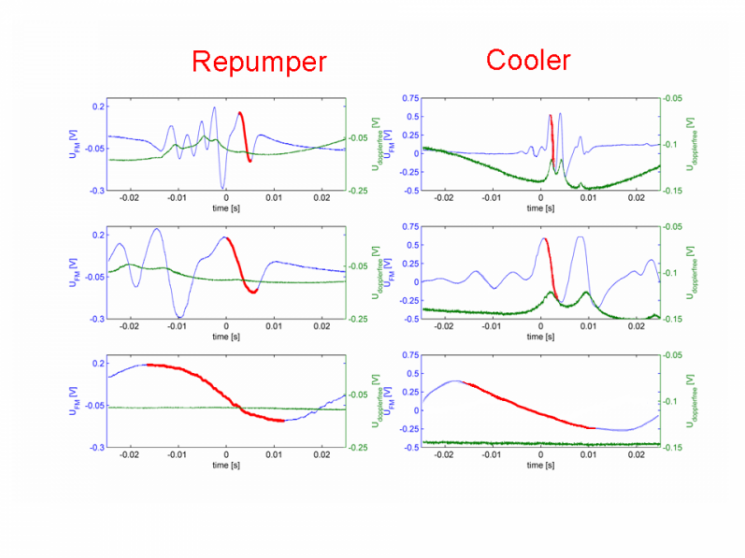

Figure 4.5: Locking the lasers to the right frequencies.

3. You should see in the signal from the slow photodiode the doppler valleys. If you don't see them change a little bit the current of the (right) laser. 5 mA should be sufficient here!

4. Use the knob at the piezo controller in order to move the right doppler valley to the center of the oscilloscope. If a mode-hop occurs, change the current of the diode laser carefully.

5. Decrease the scanning range by decreasing the gain at the PID controller carefully. You might have to correct the position of the resonance by tuning carefully the knob of the piezo controller.

6. Repeat the sequence given in 4.) until you see the right dip on the oscilloscope. Then observe the FM spectroscopy signal. Decrease the gain of your scanning range until only the correct slope is visible.

7. Switch OFF the scan by flipping the **"scan" switch** at the **PID controller** and flip ON the **"integrator"** or **"lock"** switch to lock the laser.

Note that if you hit the table or any metal part on it, it is very probable that the lasers will unlock and you'll have to lock them again.

Now it is also the right time to switch ON the Rb atoms dispenser, so, on its power supply, increase slowly the current from 0 A up to 6 A.

Magnetic coils

The cables for the magnetic coils will also be unplugged. Depending on the position of the quarter-waveplates in front of the chamber, which are preset by the tutor, the current has to flow in one or the other direction. You have to choose one direction and increase the current slowly up to a value of 6 A. In the z-Compensation coils set a current of 1 A. Pay attention that the current of the MOT coils shouldn't go over 6 A and the current of the z-Compensation coils shouldn't be higher than 2A!

Achievement of the MOT

At this point it should be possible see a MOT with the IR finger camera on the black and white TV screen, if the current in the MOT coils flows in the right direction. If you don't see a MOT, change the direction of the current, then double check the lock and the locking points of both lasers. Check also if the two irises after the fiber output are fully open. If this doesn't help, then vary the z-Compensation coils current between 0 and 2 A and try to re-balance the power between the x-y-z MOT beams by turning the lambda/2 waveplates which split the beams. With an equally split power you should see a MOT and you should see an increasing signal on the oscilloscope from the photo diode which measures the MOT fluorescence.

4.2.3 Day 3

Today you should optimize your fluorescence signal and then measure the loading characteristics of the MOT at different detunings and magnetic field gradients.

Improvement of the MOT and of the fluorescence signal

To do so you have first to adjust the photo diode to the fluorescence light emitted by the MOT by slightly improving the alignment of the mirror. (Outdated: Then maximize the signal to noise ratio using two iris diaphragms. Write down the distance of the photo diode and the opening diameter of the first iris. From this you can later on calculate the solid angle of the measured fluorescence.)

With the photo diode you now have a tool with which you can improve the MOT by increasing its fluorescence signal and you can now start to optimize it. First, play a little bit with the current of the z-Compensation coils, until you'll find the position which allows you to trap the biggest cloud with the strongest fluorescence. Then try to adjust the power balance between the

x-y-z MOT beams until you reach the highest fluorescence signal. Estimate the average laser intensity in each of the six laser beams, it should be close to 3 mW.

Don't try to optimize the fluorescence signal live by changing the alignment of the last mirrors on the beam paths, usually it leads to a complete misalignment. If you see that your atom cloud is split into two or more spots, then you should align the beams more carefully by using the masks on the viewports. Also it usually doesn't help to slightly rotate the quarter waveplates which are used to set the polarizations of the laser beams to circular because they have already been carefully optimized by the tutors.

The system is now ready for the measurements.

Why should the detuning of the laser be at a fixed value for this procedure?

Acquisition of the loading curve at different detunings and at different magnetic fields

The atom number of a MOT critically depends on the detuning and on the gradient of the magnetic trapping field. You should measure the loading curve for different configurations: vary the detuning from 14 MHz to the resonance in steps of 2 MHz with respect to the $F = 3 \rightarrow F = 4$ transition and at each detuning vary the gradient by changing the current through the quadrupole coils between 4.5A and 6A in steps of 0.5A.

The current can be easily changed by adjusting the current output of the MOT coils power supply, while you can change the detuning by adjusting the frequency of the VCO in the AOM controller via the top left knob in the frequency control area. Always measure the output frequency via the frequency counter (this device should be always set to measure Freq B). Check that the black knob in the AOM controller amplitude control area is set to 1. Set the oscilloscope to trigger on EXT in mode AUTO and set the timescale to 5 seconds.

To acquire the loading curve you should first block a MOT beam with a hand and have on the oscilloscope trace an initially flat signal corresponding to 0 atoms, then you can start the loading process by unblocking the laser beam and finally, when the signal has reached its peak value, you can save the signal on the USB drive. You have to choose the appropriate timescale to have the whole loading curve on the screen. In Fig. 4.6 a typical experimental loading curve is shown.

Where do you see the best loading rate?

For the data analysis refer to the loading curves analysis (§ 4.3.3).

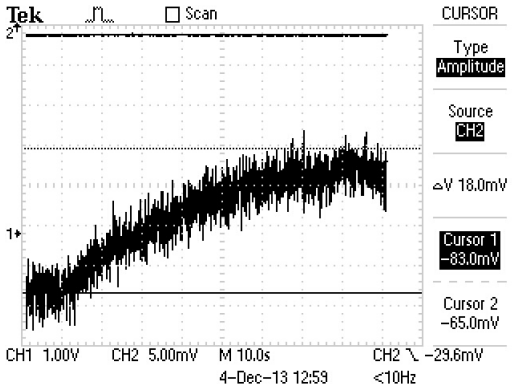

Figure 4.6: Typical experimental loading curve.

4.2.4 Day 4

If time allows, this day is reserved to do release and recapture measurements.

Release and Recapture measurement

A Release and Recapture measurement is an elegant tool to estimate the temperature of the MOT. Choose the detuning and the magnetic field gradient that gave you the best loading rate, then set the black knob in the AOM controller amplitude control area to TTL. You should start to see your MOT blinking. That's because now you are pulsing off the cooling light for a controlled time by turning off the RF power via a TTL signal on the AOM controller and this allows the atoms to freely expand during that time. When the cooling light is turned back, the atoms which weren't fast enough to escape the trapping region are recaptured in the MOT and the loading process starts again.

The frequency and duration of the pulse are controlled by a delay box which has three knobs: the first sets the time delay between one pulse and the next one, the second one allows you to fine tune the duration of the pulse on the scale set by the third knob. Set the minimum delay time and maximum width on the longest timescale. Now you should set the oscilloscope to trigger on CH1 in mode NORMAL and choose an appropriate timescale (100 ms or lower) to see on CH1 the full TTL pulse.

You should notice now that the fluorescence signal on CH2 has three distinct behaviors:

1. Initially the pulse is HIGH and you have an initial flat zone where the fluorescence signal is maximum, this is your maximum atom number;

2. When the pulse goes LOW the cooling light is turned off and there is no fluorescence from the atoms, so this is your zero atom level;

3. When the pulse goes back to HIGH, depending on the duration of the previous stage, you see either a sudden jump back to the initial level (Fig. 4.7 short pulse, nearly all atoms recaptured), or a smaller jump followed by a rising slope (Fig. 4.8 intermediate pulse, less atoms recaptured) or even a rising slope starting from the zero atom level (Fig. 4.9 long pulse, no atoms recaptured). The short initial part of this signal, just after the TTL signal on CH1 going HIGH, represents the amount of atoms which are recaptured after the time of free expansion.

You should acquire 30 traces for various durations of the pulse (i.e. duration of free expansion), taking care to set the pulse delay such that between one pulse and the other you recover your maximum atom level. The 30 traces should be composed as follows:

1. 5 traces at such short duration that you don't see a change in the atom number

2. 5 at such durations that you loose all the atoms

3. 20 traces at durations in between to sample properly the expansion behavior

From the plot of the relative atom number against the expansion time you can extract the temperature of the atoms inside the MOT through a fit, for more details on the data analysis refer to the Release and Recapture curve analysis (§ 4.3.4).

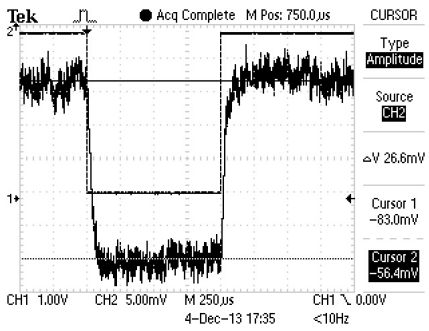

Figure 4.7: Release and recapture signal for short expansion times. A big fraction of atoms is recaptured.

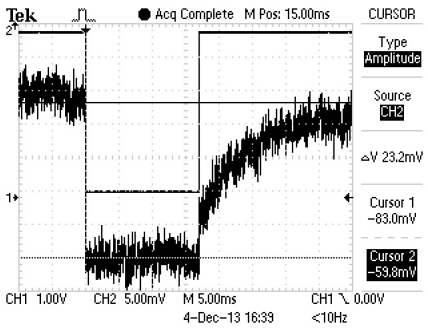

Figure 4.8: Release and recapture signal for intermediate expansion times. A smaller fraction of atoms is recaptured.

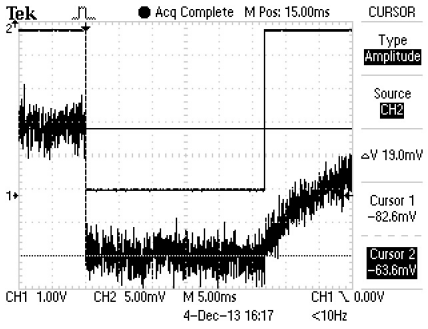

Figure 4.9: Release and recapture signal for long expansion times. No atoms are recaptured.

4.3 Data Analysis instructions

This is a set of guidelines that should help you to analyze the data and to properly report your results.

4.3.1 Opening data

The data that you acquired with the Tektronix oscilloscope is organized as follows in each folder:

- a picture of the oscilloscope screen in .jpg
- a .csv file containing the CH1 trace
- a .csv file containing the CH2 trace
- a .set file containing the oscilloscope's settings

The CSV files that contain the traces are organized in five vertical columns separated by commas ",", the time axis values are stored in the fourth column, while the voltages are in the fifth, so when importing these files in your data analysis program you should set the comma as the column separator. Additionally the first 19 rows have the oscilloscope settings written in the first three columns, so either you skip these lines or you take this fact into account when importing your data.

4.3.2 Spectroscopy

You should have recorded the spectrum of both cooler and repumper lasers and you have to analyse only the best set between the two.

For all these datasets, to perform the frequency measurements you have to calibrate the horizontal axis, by converting it from time to frequency. To do so you should choose a set of two lines as distant as possible and equate their time separation to their theoretical frequency separation, then use this linear relationship as your calibration. For the hyperfine frequency separation datasets it is wise to use the crossover lines, in order to be able to measure the separation between the real transitions. If you maintain the scanwidth setting on the PID controller for few datasets, then you can do the calibration once on one of these datasets and use it also for the others, allowing you to measure the frequency of all lines not used for the calibration and to compare them with the theoretical expectation.

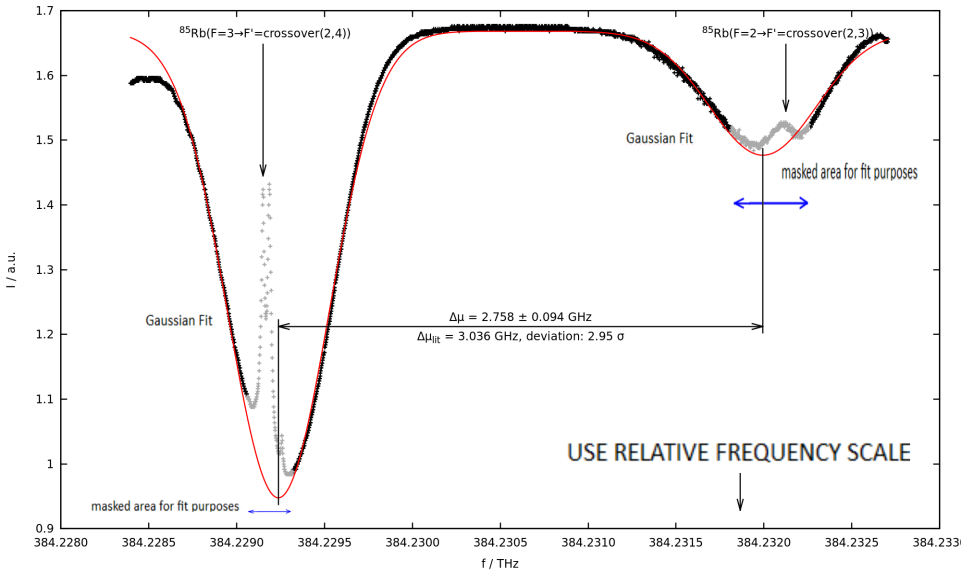

Figure 4.10: Example Multiplet separation.

Multiplet separation

- $^{87}Rb\ F = 2 \rightarrow F'$ and $^{85}Rb\ F = 3 \rightarrow F'$ transitions
- $^{85}Rb\ F = 3 \rightarrow F'$ and $^{85}Rb\ F = 2 \rightarrow F'$ transitions
- $^{85}Rb\ F = 2 \rightarrow F'$ and $^{87}Rb\ F = 1 \rightarrow F'$ transitions

Analyse these datasets by fitting each absorption profile with a Gaussian and then compare the distance between the centers with the theoretical multiplet separation. To have a better fit, it is suggested to mask the areas where the Lorentzian dips are. An example of the analysis is shown in Fig. 4.10.

Natural transition line width and Doppler Broadening

- $^{87}Rb\ F = 2 \rightarrow F'$ transitions
- $^{85}Rb\ F = 3 \rightarrow F'$ transitions
- $^{85}Rb\ F = 2 \rightarrow F'$ transitions
- $^{87}Rb\ F = 1 \rightarrow F'$ transitions

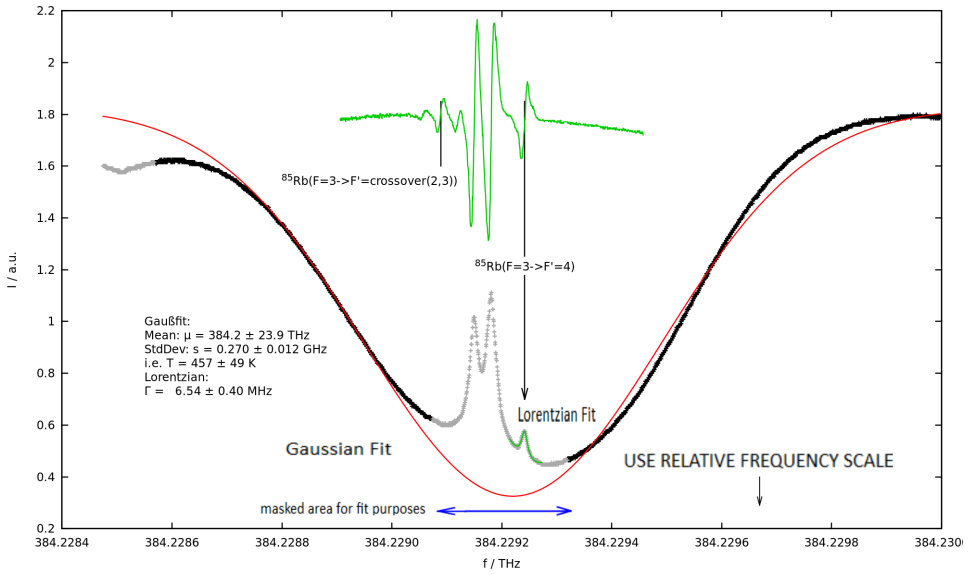

Figure 4.11: Example Natural transition line width and Doppler Broadening analysis.

From these datasets you can then measure the **line width** of the **hyperfine lines** and the **Doppler valley**. You have to fit each absorption profile with a Gaussian, subtract it, then fit the real absorption dips with a Lorentzian (only the ones that have a good SNR). To have a better fit, it is suggested to mask the areas where the Lorentzian dips are. Extract from the FWHM of the Doppler valleys the temperature of the atomic sample and compare it with the Doppler broadening expected for a thermal gas. From the Lorentzian fit extract the line width and compare it to the theoretical natural line width of the transitions. An example of the analysis is shown in Fig. 4.11.

Hyperfine splitting

- $^{87}Rb\ F = 2 \rightarrow F'$ transitions
- $^{85}Rb\ F = 3 \rightarrow F'$ transitions
- $^{85}Rb\ F = 2 \rightarrow F'$ transitions
- $^{87}Rb\ F = 1 \rightarrow F'$ transitions

From these **recorded Doppler free spectra** you can measure the D2 line hyperfine energy level separation (§ 1.6.2). You need to find in the

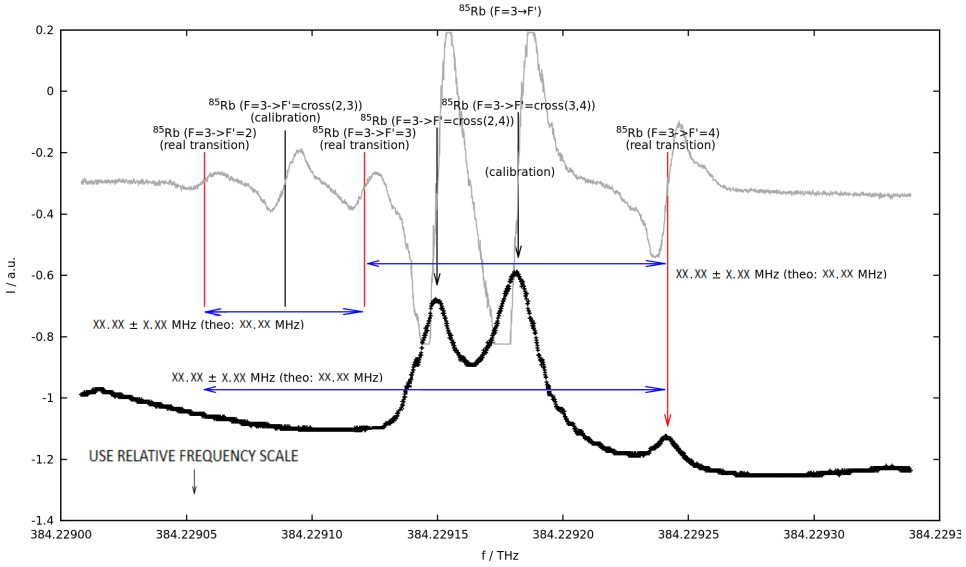

Figure 4.12: Example Hyperfine splitting analysis.

derivative the six zero crossings and you have to compare their frequency separation (**it's a relative frequency measurement!**) with the theoretically expected frequency separations between the hyperfine transitions. An example of the analysis is shown in Fig. 4.12.

4.3.3 Loading Curves

As a first step of the data analysis, convert the measured voltage into the number of atoms following this conversion guide (§ 4.3.5). Take into account that the initial flat zone corresponds to zero atoms. From the Loading Process theoretical model (§ 2.5) you learned that you have to fit each loading curve (like in Fig. 4.13) with the solution of the following rate equation:

$$\frac{dN}{dt} = L - \alpha N \tag{4.1}$$

Study the loading rate, the one body loss coefficient and the final atom number as a function of the detuning and as a function of the magnetic field gradient (Fig. 4.14, 4.15 and 4.16). Remember that the MOT coils have 90 windings and a diameter of 17 cm. Finally summarize your results with a 3D plot showing the final atom number as function of the detuning and of the magnetic field gradient, like in the Fig. 4.17.

Are the loss coefficients constant? What would it mean if they were dependent on the atom number? What is the behavior in detuning?

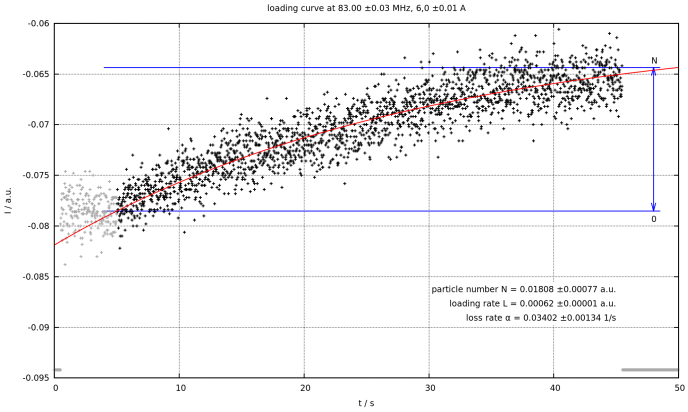

Figure 4.13: Example loading curve fit.

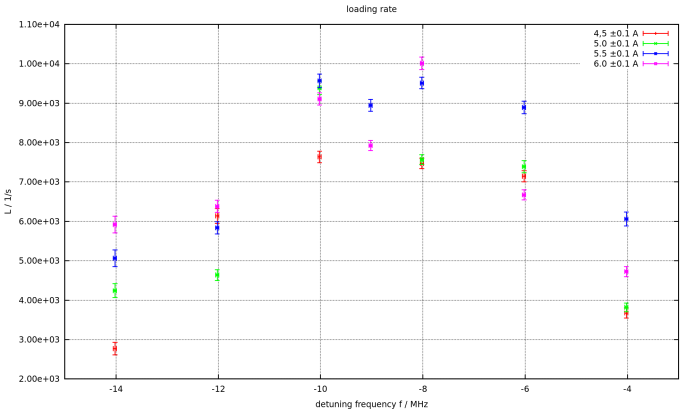

Figure 4.14: Example loading rate plot.

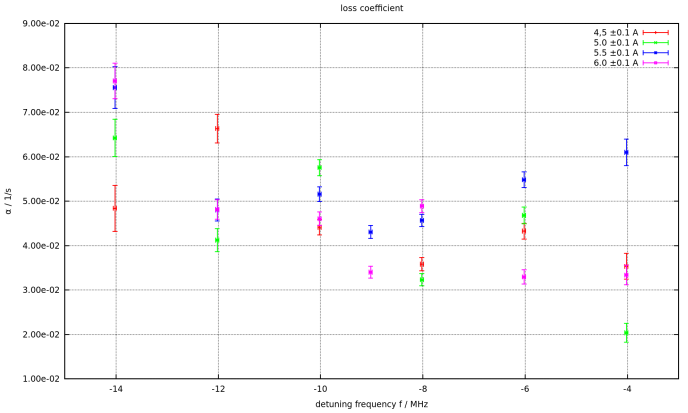

Figure 4.15: Example loss rate plot.

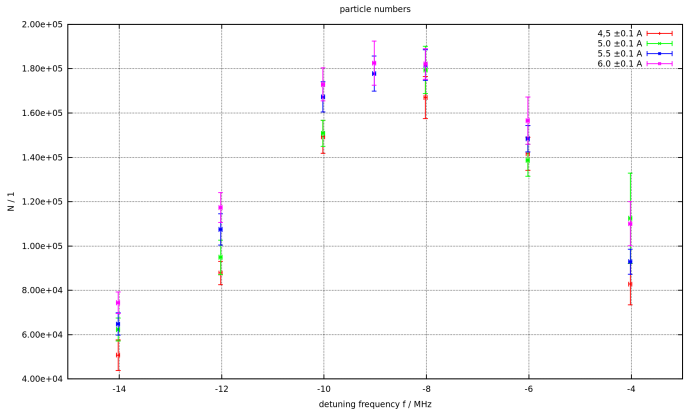

Figure 4.16: Example maximum loaded atom number plot.

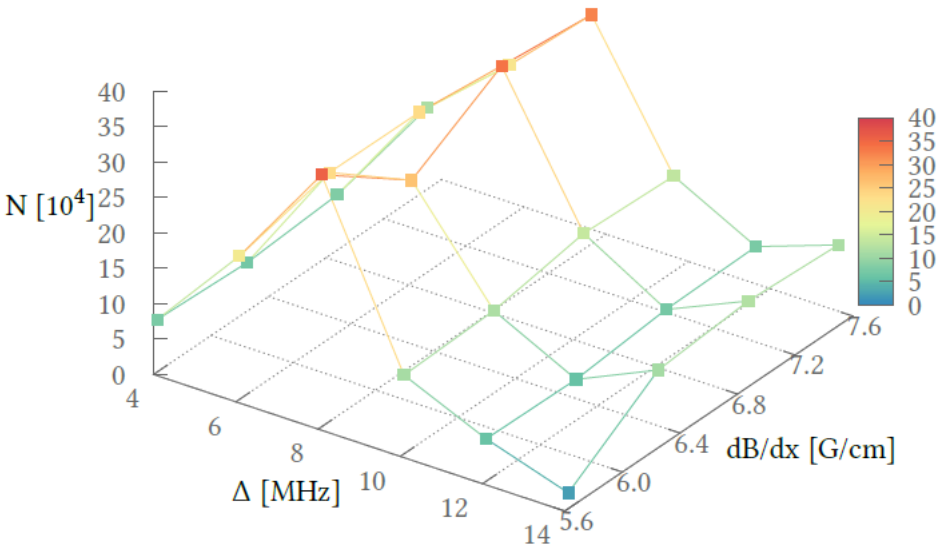

Figure 4.17: Example 3D summary plot.

4.3.4 Release and Recapture

From the acquired traces extract the maximum atom number and the number of atoms recaptured after the free expansion time, paying attention that:

- When initially the CH1 pulse is HIGH you have in CH2 an initial flat zone where the fluorescence signal is maximum, so an average over this part represents your maximum atom number;
- When the pulse goes LOW the cooling light is turned off and there is no fluorescence from the atoms, so this is your zero atom level;
- When the pulse goes back to HIGH, depending on the duration of the previous stage, you see either a sudden jump back to the initial level, or a smaller jump followed by a rising slope or even a rising slope starting from the zero atom level. The short initial part of this signal, just after the TTL signal on CH1 goes HIGH, represents the amount of atoms which are recaptured after the time of free expansion, so average over it to extract this value.

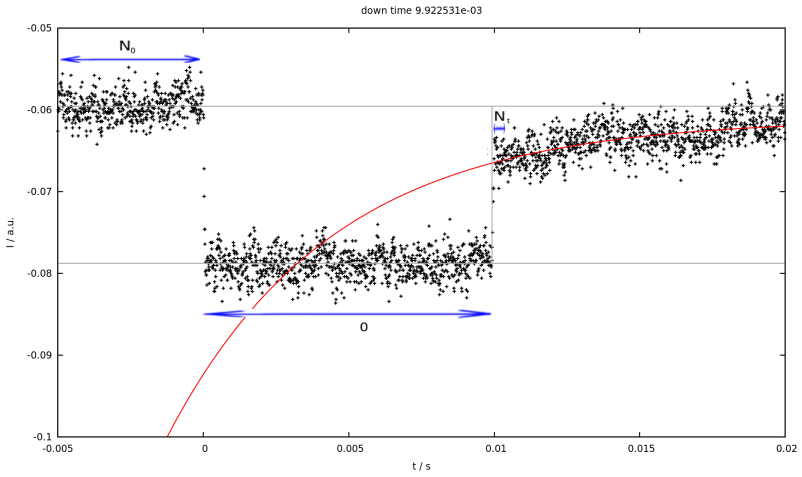

Figure 4.18: Example raw release and recapture trace.

In Fig. 4.18 there is an example of such analysis. For these measurement is not important to convert from volts to atom number since you have to perform a relative measurement, just take properly into account the zero atom voltage level.

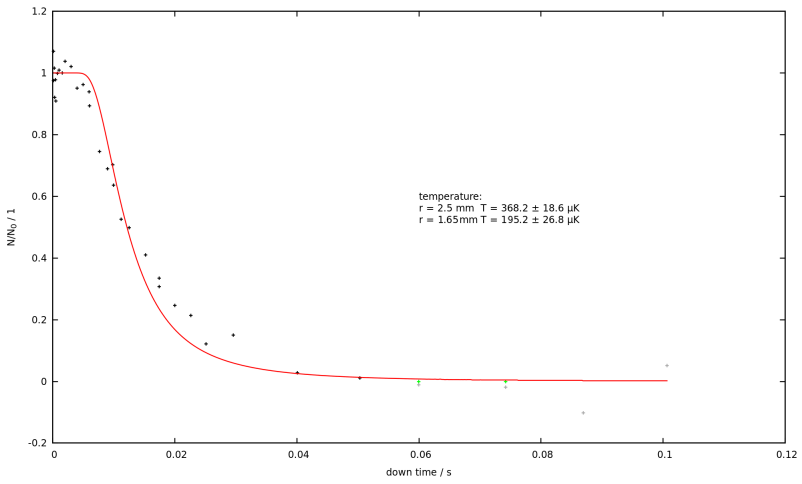

Figure 4.19: Example Release and Recapture fit.

From the plot of the relative atom number against the expansion time (Fig. 4.19) you can extract the temperature of the atoms inside the MOT by fitting the following function:

$$\frac{N(t)}{N(0)} = erf(\chi) - \frac{2}{\sqrt{\pi}}\chi e^{-\chi^2} \tag{4.2}$$

where $\chi = \sqrt{\frac{M}{k_B T}}\frac{R}{t}$ and use as MOT radius R=1.5 mm. The theory behind this fitting function is described in the theory chapter Temperature measurement via release and recapture (§ 2.7).

Is the calculated temperature compatible with the one that you expected to achieve?

4.3.5 Conversion from Volts to Atom Number

In order to convert the voltage signal measured by the photodiode into the number of atoms captured in the MOT you have to perform few steps.

The atoms absorb light from the laser beams and re-emit this light with a rate given by the **Scattering rate** (pay attention that this rate depends on the detuning of the laser beams!):

$$\Gamma_{sc}(\Delta) = \frac{\Gamma}{2}\frac{I(r)/I_{sat}}{1 + I(r)/I_{sat} + 4\Delta^2/\Gamma^2} \tag{4.3}$$

where the natural line width is $\Gamma(^{85}Rb) = 2\pi 6.07 MHz$ and $I_{sat} = \frac{2\pi^2\hbar\Gamma_c}{3\lambda_c^3} = 4.1 mW/cm^2$ for randomly polarized light (this gives the best estimation according to [10]).

You should approximate $I(r)$ with the intensity in the center of the beam I_0 and consider that the atoms are illuminated by six laser beams. The relationship between I_0 and the six beam total power measured on the power meter is $I_0 = 2P_{powermeter}/\pi w^2)$, considering a Gaussian beam profile of the beams with waist $w = 2.0mm$.

The next step is to consider that the atoms spontaneously emit isotropically, so the total emitted power by N_{atoms} is:

$$P_{emitted} = \Gamma_{sc}(\Delta)E_\nu(\lambda)N_{atoms} \tag{4.4}$$

where $E_\nu(\lambda) = \frac{hc}{\lambda}$.

Of this total power we collect only a small fraction with our imaging system because we observe only a small **solid angle**, limited by the distance from the atoms and the radius of the collecting lens ($r = 25.4mm$):

$$P_{meas} = \theta_\Omega P_{emitted} \tag{4.5}$$

with the solid angle $\theta_\Omega = \frac{\pi r^2}{4\pi d^2}$. Our imaging system (see Fig. 4.20) is made by a simple single lens positioned at a distance of 2 focal lengths away from the MOT in order to form a 1:1 image on the photodiode. Since $f = 75mm$, then $d = 150mm$.

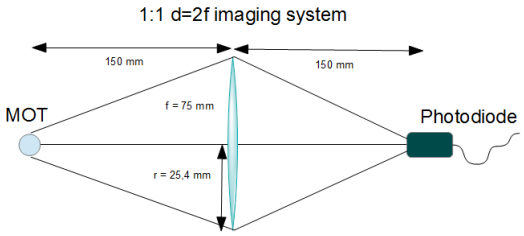

Figure 4.20: MOT fluorescence imaging system.

Finally this power is measured by a Thorlabs photodiode PDA36A which converts it into voltage:

$$V_{out} = P_{meas}QE(\lambda)GST \tag{4.6}$$

where $T = 0.96$ is the transmission through the optical viewport, $G = 4.75 * 10^6 V/A \pm 5\%$ is the gain of the photodiode amplifier (when set to $+70dB$) and the Quantum Efficiency of the sensor is $QE \approx 0.52 \pm 0.015 A/W$. $S = \frac{R_{load}}{R_{load}+R_s}$ is the scale factor given by the voltage divider between the input impedance of the oscilloscope $R_{load} \geq 1M\Omega$ and the output resistor of the photodiode $R_s = 50\Omega$.

Combining the previous formulas together we finally get the **detuning dependent conversion factor** from Volts to Atom Number:

$$N_{atoms}(\Delta) = \frac{V_{out}}{QE(\lambda)GST\theta_{\Omega}\Gamma_{sc}(\Delta)E_{\nu}(\lambda)} \tag{4.7}$$

Bibliography

[1] Interaction in Ultracold Gases: From Atoms to Molecules; M. Weidemüller and C. Zimmermann; Wiley-VCH, 1st edition Mai 2003

[2] D. Wineland and H. Dehmelt, Bull. Am. Phys. Soc. 20, 637 (1975).

[3] T. Hänsch and A. Schawlow, Cooling of Gases by Laser Radiation, Opt. Commun. 13, 68-71 (1975)

[4] H. Metcalf and P. van der Straten, Laser cooling and trapping of atoms; JOSAB 20, 887 (2003)

[5] S. Chu et al., "Three-dimensional viscous confinement and cooling of atoms by resonance radiation pressure", Phys. Rev. Lett. 55 (1), 48 (1985)

[6] P. D. Lett et al., "Optical molasses", J. Opt. Soc. Am. B 6 (11), 2084 (1989)

[7] E. Raab et al.,Trapping of neutral-sodium atoms with radiation pressure, Phys. Rev. Lett. 59, 2631 (1987)

[8] L. Ricci, M. Weidemüller, T. Esslinger, A. Hemmerich, C. Zimmermann, V. Vuletic, W. König, T. W. Hänsch, A compact grating-stabilized diode laser system for atomic physics, Opt. Comm. 117, 541-549 (1995)

[9] C. Wieman and L. Hollberg, Using diode lasers for atomic physics, Rev. Sci. Inst. 62 (1991)

[10] H. J. Lewandowski, D. M. Harber, D. L. Whitaker, and E. A. Cornell, Simplified System for Creating a Bose-Einstein Condensate, J. Low Temp. Phys. 132, 309 (2003)